Tribology International 175 (2022) 107804

Contents lists available at ScienceDirect

Tribology International

journal homepage: www.elsevier.com/locate/triboint

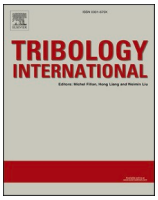

Comparison of sustainable cooling systems used in the drilling repair of Mg-Al and Mg-Ti multi-material parts in the aeronautical industry

David Blanco [a,1,*], Eva María Rubio [a], María Ana Sáenz-Nuño [b], Raquel María Lorente-Pedreille [b]

[a] Department of Manufacturing Engineering, Industrial Engineering School, Universidad Nacional de Educación a Distancia (UNED), St. Juan del Rosal 12, E28040 Madrid, Spain
[b] Institute for Research in Technology (IIT) – ICAI School of Engineering, Comillas Pontifical University, St. Alberto Aguilera, 25, E28015 Madrid, Spain

ARTICLE INFO

Keywords:
Multi-material
Machining
Cooling
Sustainable

ABSTRACT

The article presents as a novelty a comparative study of the efficiency of different sustainable cooling systems in the re-drilling repair process of magnesium-based multi-material components for aeronautical and automotive sectors. The cooling systems compared are: *dry machining, minimum quantity of lubricant with eco-fluid (MQL-Eco), cold compressed air (CCA) and cryogenic machining.* Multi-materials used are magnesium-aluminium and magnesium-titanium combinations. The study uses descriptive statistics and ANOVA to conclude the significant factors and interactions. Conclusions highlight differences depending on the type of response variable chosen. The best results for the *Mg-Al-Mg* are obtained using *MQL-Eco*, and for *Mg-Ti-Mg* with *cryogenic machining.*

1. Introduction

Sustainable development and energy efficiency are currently key targets for the development of the technological and industrial areas. According to the reports of the Intergovernmental Panel on Climate Change (IPCC), humans have a clear influence on global warming. Emissions resulting from the use of fossil fuels are among the causes for the 40 % increase in carbon dioxide emissions compared to the pre-industrial era. In addition, the oceans have absorbed about 30 % of the carbon dioxide emitted, resulting in their acidification [1]. Climate warming due to human activities is currently calculated to increase by 0.2 °C per decade and, to stabilise, global net CO_2 emissions from human activities would need to reach net zero by 2050 [1,2]. Transport is estimated to be responsible for more than 30 % of CO_2 emissions in the European Union (EU). As a result, the EU has committed to reducing transport emissions by 60 % by 2050 compared to 1990 levels [3]. On the other hand, progressive stricter legislation is foreseen on CO_2 emission limits in all sectors, particularly in the road [3], air [4] and maritime transport [5], aiming to achieve a reduction in emissions that will stabilize global warming at 1.5 °C above pre-industrial levels. In this context, major aircraft companies like Boeing [6] and Airbus [7] are undertaking significant efforts to move towards sustainability and emissions reduction. For example, each new generation of Boeing aircraft is up to 25 % more efficient than the previous one [8] and, in the case of Airbus, the A350 model is made of 53 % lightweight structural materials and is capable of saving up to 25 % fuel compared to the previous model, while the A220 family of aircraft is the most efficient in its class [9]. Over the next 20 years, more than 12,000 aircraft are expected to reach the end of their life. Therefore, the development of techniques and materials that enable their recycling or reuse is another key line of development towards sustainability. Since 2007, Airbus has recycled 117 aircraft, with 92 % of parts reused and 100 engines fully recycled [10]. In addition, energy efficiency and pollutant emissions are directly linked to the mass of automobiles [11] and aircraft [8,9] For this reason, an important research line aims at reducing the mass of transport vehicles by using lightweight structural materials and light metal alloys [12]. Important lightweight candidates to replace conventional materials employed for transport vehicles are high-strength steels [13,14], aluminium alloys [15,16], titanium alloys [17], magnesium alloys [18,19] and polymers [20,21]. In addition, these lightweight structural materials can be used combined or with other lightweight and strong materials to create multi-material structures. These hybrid structures provide better strength-to-mass ratios, while maintaining good wear and fatigue properties, and are one of the trending topics in studies related to

* Corresponding author.
E-mail addresses: dblanco78@alumno.uned.es (D. Blanco), erubio@ind.uned.es (E.M. Rubio), msaenz@iit.comillas.edu (M.A. Sáenz-Nuño), rmlorente@icai.comillas.edu (R.M. Lorente-Pedreille).
[1] Programa de Doctorado en Tecnologías Industriales

https://doi.org/10.1016/j.triboint.2022.107804

Available online 23 July 2022

lightweight structural materials applied to the aeronautical, aerospace and automotive sectors [12].

Aluminium alloys are characterised by their lightweight, corrosion resistance, and good thermal and electrical conductivities [15]. For this reason, they are the lightweight structural materials that appear in most recent studies, either as individual materials or as multi-material composites [12]. In addition, they are frequently used in the aeronautical, aerospace and automotive sectors [15,17,22]. The transport sector consumes 35–40 % of the aluminium alloys manufactured [23]. It is also frequently used in combination with other materials to form multi-material components such as aluminium and steel [24], fibre reinforced polymers (FRPs) [25], magnesium alloys [26] or titanium alloys [17].

Titanium alloys have very good structural properties thanks to their metallographic structure. Among them stand out their lightweight, high wear and corrosion resistance, and their capacity to maintain a good resistance at high temperatures. Therefore, titanium alloys are widely employed in industries such as aerospace, aeronautics, automotive and biomedical [27,28]. However, titanium alloys are considered to be materials very difficult to machine because of their low thermal conductivity, low modulus of elasticity and high chemical affinity with tool materials. This causes excessive wear of the tool during machining, increasing its cost [20,29–32], and makes it frequent to study sustainable cooling techniques to achieve the surface roughness required by the sector in which they will be employed [30]. Machining processes that have better surface finishing produce higher compressive residual stresses from machining that are positive in terms of the fatigue strength of the component [33,34].

On the other hand, magnesium alloys are the lightest structural alloys on the planet. However, their formability is far below other light alloys, such as aluminium. This low formability is determined by their hexagonal metallographic structure [19,35]. For example, cracks and fissures appear in pure laminated polycrystalline magnesium when reducing the thickness by approximately 30%. Ideally, it is possible to develop new magnesium alloys, but so far, no super-conformable magnesium alloy has been obtained at room temperature. However, recent studies indicate that if the grain size is reduced on a microscopic scale by severe plastic deformation, grain boundary slips can be activated to improve ductility [36–38]. This effect can be applied to other materials with hexagonal crystallographic structures. On the other hand, magnesium alloys generate low temperatures and forces during machining, and their chips are short. This fact results in a long tool life, which can be increased if sustainable lubrication/cooling techniques are applied during the machining process. Both magnesium [39] and aluminium [40] have good recyclability. Moreover, studies involving hybrid components are identified as current trending research areas. Among them, the most studied combination of material types over the last few years is the metal + metal combination [12,22]. Based on the previous information, it is concluded that the optimisation and understanding of sustainable machining processes applied to magnesium-based multi--materials, such as *Mg-Al-Mg* and *Mg-Ti-Mg*, are topics of current scientific interest, with a potential direct application in the aeronautical, aerospace and automotive sectors.

On the other hand, within the field of multi-materials, one of the most studied topics is the problem of joining different materials. The main joints are mechanical, by drilling and subsequent bolting or riveting [11,20], chemical, using adhesives [41,42], and thermal, through different welding technologies [13,43].

Drilling is involved in 50 % of machining operations [44] and it is the most frequent machining process for mechanical assembly operations [17,31,45–47]. In the case of multi-material drilling, a single machining operation is a challenge because of the different characteristics of the individual materials. This often requires the use of compromises in cutting conditions and frequently leads to associated problems such as severe tool wear, increased cutting forces, poor hole quality or large burrs, aggravating difficulties at the materials interface [20,43]. In the case of titanium, chips in multi-material compounds can cause scratches at the materials interface and during chip evacuation. In addition, the number of holes drilled has an influence on the surface quality obtained because of the tool wear effect [20]. On the other hand, the holes drilled in aeronautical components to assemble the various parts are subject to cyclical stresses and this can lead to fatigue failures. The processes related to drilling are little studied regarding fatigue as they have not been considered critical so far. In addition, it is very difficult to investigate the surface texture of holes and the residual stress fields. Recently, some problems caused by increasing thermo-mechanical loads have been detected in some critical parts linked to the automotive or aeronautical sectors, such as crankshafts or turbines, and therefore they are attracting researchers' attention [48]. Given the responsibility of the parts, they must be subjected to frequent maintenance checks and repair of potential cracks that could result in catastrophic failure of the part during service [17]. On the other hand, there is a constant drive to find new and innovative ways for industry to reduce its impact on the environment. Efforts are currently focused on: efficient resource consumption and energy conservation, minimising the environmental effects of energy production, improving the waste management system, and improving the environmental impact of energy production [49,50]. Regarding this point, the choice of cooling strategy is an important issue concerning the sustainability of machining processes. This choice is of great importance as it affects the friction between tool and chip, the lubrication degree in the contact zone between the workpiece and the tool, the process temperature and the chip evacuation [17,51]. Lubricants and cutting fluids (CFs) represent approximately 17% of the machining costs, and tool costs account for 4 % [28,48,52]. These fluids include in their composition chemical components that are harmful to the environment and human beings; in the case of humans, they can cause respiratory problems, asthma and cancer [28,49,53]. For this reason, the current trend in recent studies related to the optimisation of machining processes is the use of sustainable cooling/lubrication techniques. This is the case of dry machining [17,26,28,33,35,54,55], cryogenic cooling [27,28,54,56], minimum quantity lubrication (MQL) [27,28,35,48,50,57–59], cold compressed air [60–62] and the use of sustainable cutting fluids based on vegetable oils such as sesame, coconut, sunflower, palm and others [28,32,63]. García-Martínez et al. [28] carried out in 2018 an interesting analysis of recent literature related to non-traditional lubrication techniques developed for turning, drilling and milling processes. The study includes scientific literature published from 2015 onwards. The paper concludes that cryogenic lubrication can improve the surface quality of machined parts; therefore, this technology is considered to have the potential to replace traditional flood lubrication. However, the conclusions on tool wear are not so clear, since, although in some works an improvement in tool life is reported, in others there is an increase in wear tool and cutting forces related to the increase in Ti hardness at low temperatures. Therefore, MQL appears to many authors as a good compromise solution that reduces the amount of coolant and achieves the same or better surface roughness results than conventional cooling. In 2015, Carou et al. [57] conducted a review of representative studies on the use of the MQL system in the turning of the main materials involved in the aeronautical sector: nickel-based alloys, steels and light metals, including aluminium alloys, magnesium alloys and titanium alloys.

Cryogenic machining (CM) a highly efficient machining technique that uses a cryogenic coolant to decrease the temperature at the chip-tool interface, reducing tool wear or changing the material characteristics and thereby improving machining performance and product quality. Some of the interesting advantages are: reduced chip-tool interface temperature, reduced tool wear, higher production rates, higher product quality, energy savings, no wet chips, no contaminated parts or disposal costs, and the disadvantages are the additional equipment costs and the high price of liquid nitrogen, which is not reusable [50]. In 2018, Suhaimi et al. [27] proposed a new tool design that allows cooling by an internal cryogenic nitrogen circuit. In this way, the

Table 1
Factors and levels.

Factors	Levels (code)	Levels (values)	Type
Tool	*t1*	*Güring HSCO*	Qualitative
Depth of cut, *ap, (mm)*	*d1*	*0.15*	Quantitative
Feed rate, *f (mm/rev)*	*f1*	*0.1*	Quantitative
Spindle speed *N (rev/min)*	*N1*	*850*	Quantitative
	N2	*1000*	
Cooling system, *C*	*Dry machining*	*C1*	Qualitative
	MQL + Eco	*C2*	
	Cold compressed air	*C3*	
	Cryogenic machining	*C4*	
Specimens, *S*	*Mg-Al-Mg*	*S1*	Qualitative
	Mg-Ti-Mg	*S2*	
Location regarding insert, *LRI*	*Mg1 / Al2 / Mg3*	*LRI1*	Qualitative
	Mg1 / Ti2 / Mg3	*LRI2*	
		LRI3	
Location regarding specimen, *LRS*	*Drill hole at entry*	*LRS1*	Qualitative
	Drill hole at exit	*LRS2*	
Measurement zone	*Zone 1* (From 0–2 mm)	*Z1*	Qualitative
	Zone 2 (From 2–6 mm)	*Z2*	

Table 2
Experimental design carried out on *S1* and *S2* specimens.

Test	1	2	3	4	5	6	7	8
LRI / LRS	*LRI1*	*LRI1*	*LRI1*	*LRI1*	*LRI1*	*LRI1*	*LRI1*	*LRI1*
	LRS1	*LRS1*	*LRS1*	*LRS1*	*RS1*	*LRS1*	*LRS1*	*LRS1*
	LRI1	*LRI1*	*LRI1*	*LRI1*	*LRI1*	*LRI1*	*LRI1*	*LRI1*
	RS2	*LRS2*	*LRS2*	*LRS2*	*LRS2*	*RS2*	*LRS2*	*LRS2*
	LRI2	*LRI2*	*LRI2*	*LRI2*	*LRI2*	*LRI2*	*LRI2*	*LRI2*
	LRS1	*LRS1*	*LRS1*	*LRS1*	*LRS1*	*LRS1*	*LRS1*	*LRS1*
	LRI2	*LRI2*	*LRI2*	*LRI2*	*LRI2*	*LRI2*	*LRI2*	*LRI2*
	LRS2	*LRS2*	*LRS2*	*LRS2*	*LRS2*	*LRS2*	*LRS2*	*LRS2*
	LRI3	*LRI3*	*LRI3*	*LRI3*	*LRI3*	*LRI3*	*LRI3*	*LRI3*
	LRS1	*LRS1*	*LRS1*	*LRS1*	*LRS1*	*LRS1*	*LRS1*	*LRS1*
	LRI3	*LRI3*	*LRI3*	*LRI3*	*LRI3*	*LRI3*	*LRI3*	*LRI3*
	LRS2	*LRS2*	*LRS2*	*LRS2*	*LRS2*	*LRS2*	*LRS2*	*LRS2*
Cooling System, C	*C1*	*C1*	*C2*	*C2*	*C3*	*C3*	*C4*	*C4*
N (rev/min)	*N1*	*N2*	*N1*	*N2*	*N1*	*N2*	*N1*	*N2*

temperature of the workpiece to be machined is kept at its working standard, preventing hardening. In another article, Sun et al. [30] present a study on machining forces, finishing surfaces and tool wear for Ti-5553 alloy. They employ cryogenic cooling and compare these results with flood and MQL cooling. In the experimental test conducted, machining forces are reduced by 30% when using cryogenic cooling compared to MQL; although MQL cooling achieves better finishing as it is more ductile at higher temperatures. On the other hand, surface roughness increases when the feed rate increases for the three types of cooling compared, cryogenic, MQL and flooding. In 2020, Gupta et al. [54] also carried out a comparative study of the most popular sustainable cooling systems for difficult-to-machine materials; dry machining, cryogenic cooling, and a combination of cryogenic cooling with MQL. The hybrid process provides cooling to the workpiece and tool and, at the same time, lubricates the cutting zone; protecting the machine from vibration and wear. The research team concludes that liquid nitrogen (LN2) + MQL hybrid cooling produces the best results of the three types of environmentally friendly cooling compared, reducing total machining cost up to 65.84 %, energy consumed 15.89 %, carbon emissions, cutting force values, surface roughness and cutting temperature [54,64]. On the other hand, there is also another research line that seeks to promote the use of sustainable cutting fluids based on biodegradable vegetable oils like sesame, coconut, sunflower or palm oil, just to mention the most relevant ones [28]. In 2016, Singaravel et al. published a study [63] on the application of vegetable oil-based dielectric fluids in machining by electrical discharge machining (EDM) and compared the surface roughness results obtained with those obtained using conventional dielectric fluids. For this purpose, the authors perform machining tests on Ti-6Al-4V specimens and use sunflower, colza and jatropha oils as biodegradable dielectric fluids and paraffin as conventional dielectric fluid for comparison. The study concludes that it is viable to use successfully sustainable biodegradable oils. These oils have similar dielectric properties and erosion mechanisms to conventional dielectric fluids, making them a promising option for sustainable manufacturing.

On the other hand, models of classical statistical experiments that aim to determine the influence of the factors on the variable of interest by varying one factor per test consume a lot of time and economic resources, and do not allow to know the interactions between factors. The application of design of experiments methodologies solves these drawbacks and optimizes the information obtained from experimental tests. This methodology is based on models that use statistical techniques such as analysis of variance (ANOVA), which allow knowing the factors of influence, their percentage of influence and the interactions between factors [21,26,46,59,65]. The most widely employed equipment to analyse the surface quality in machining processes is the roughness profilometer, a device that performs a statistical analysis based on measurements taken by contact. The main elements that compose a roughness metre are the measuring head, which touches the surface of a part to measure roughness; the transducer, a device that obtains the physical information and transforms it into electrical signals or pulses; and a calculator, which performs the mathematical calculation of the lengths, heights and widths of the profile according to the parameter being evaluated to give the degree of roughness in microns [47]. Among the two-dimensional parameters most commonly used in machining processes are the *arithmetical mean deviation, Ra*, and the *maximum peak to valley height of the profile, Rz* [66,67]. *Ra* is the arithmetic mean value of the filtered roughness profile, calculated from the deviations from the centre line within the assessment length, and it the most popular parameter for a machining process and product quality control, *Rz* is the average peak-to-valley height; smoothes out major deviations that are not representative of the surface finish [68]. In the case of aeronautical applications, a frequently applied range to define surface roughness limits is $0.8\ \mu m < Ra < 1.6\ \mu m$ [69]. However, two-dimensional profile parameters have a strong dependence on the direction chosen for the measurement and therefore have important constraints. For this reason, there is a growing trend towards the use of measurement technologies that analyse areas rather than profiles. These technologies provide a better overview. However, they are not yet widely deployed in industrial process follow-up because of the current lack of experience in their use and the lack of existing references for the definition of manufacturing tolerances. Both technologies evaluate roughness by analysing particular geometry characteristics and processing the data obtained using statistical techniques.

Among the parameters employed for area measurements is the *arithmetic mean of the absolute values of the deviations of the surface from the median plane, Sa*, and the *height from the peak to the valley of the surface, Sz*. For several reasons, the profile and area measurements do not have a direct correlation. It is worth highlighting the fact that the area information is more complete because it evaluates also the peaks and valleys of the sampling area; whereas a measurement taken following a profile does not consider these values. Furthermore, the filters applied when processing profile and area data are different [70,71]. From the previous information, it can also be concluded that the comparative study between conventional profile assessment technologies and the new areal assessment technologies is currently of scientific interest. This makes it possible to evaluate the relationship between the two types of measurement and provides a deeper surface characterisation. Furthermore, it is highly interesting to find manufacturing tolerances and references to enable, in the future, the use of these new

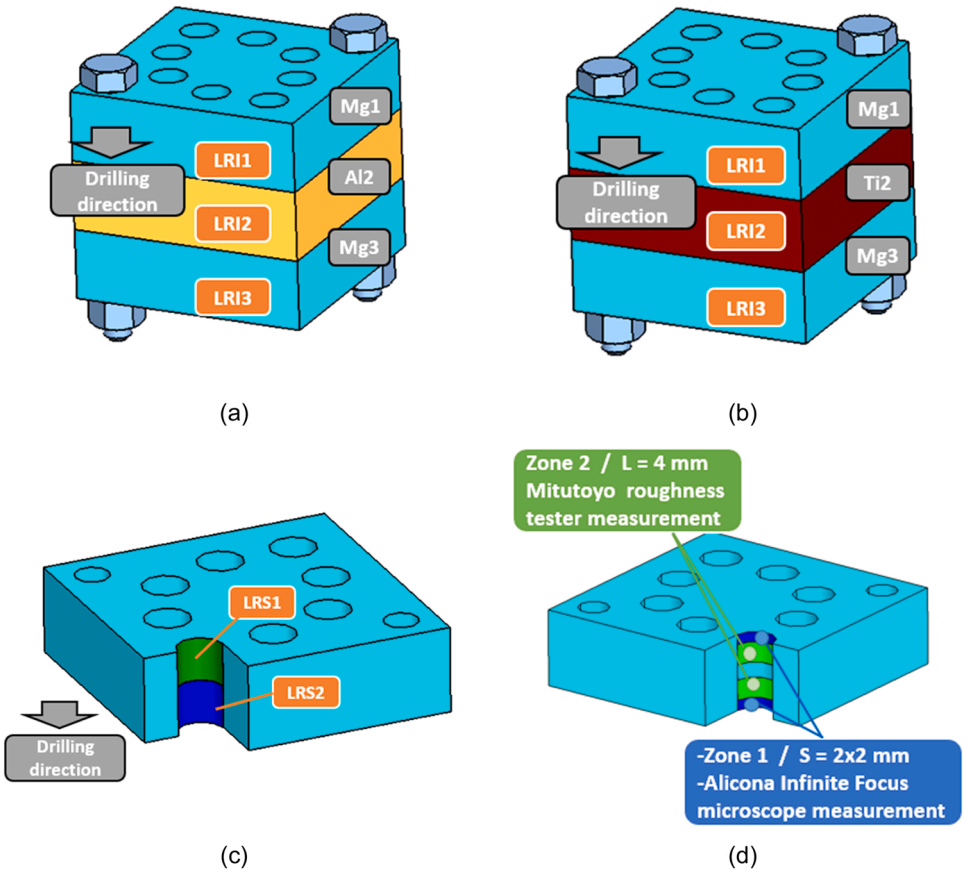

Fig. 1. Factors and levels for LRI and LRS in specimens Mg-Al-Mg and Mg-Ti-Al: (a) location regarding insert, LRI in Mg-Al-Mg; (b) location regarding insert, LRI in Mg-Ti-Mg; (c) location regarding specimen, LRS for both specimens; (d) Zones 1 and 2 inside each hole and measurement equipment used.

Table 3
Videos of each re-drilling test conducted on the multi-material specimens according to preset machining conditions and type of sustainable cooling.

Test per specimen	1	2	3	4	5	6	7	8
Cooling System, C	*C1*	*C1*	*C2*	*C2*	*C3*	*C3*	*C4*	*C4*
N (rev/min)	*N1*	*N2*	*N1*	*N2*	*N1*	*N2*	*N1*	*N2*
Mg-Al-Mg	1.1	1.2	1.3	1.4	1.5	1.6	1.7	1.8
Mg-Ti-Mg	2.1	2.2	2.3	2.4	2.5	2.6	2.7	2.8

measurement technologies for process quality control.

This work continues a previous research project in which the recent literature associated with multi-materials and structural lightweight materials has been reviewed [22,67,72], a suitable tool has been selected for the re-drilling of the most demanding multi-material *Mg-Ti-Mg* [35], the best process parameters for the re-drilling of *Mg-Ti-Mg* [17] and *Mg-Al-Mg* [73] specimens by dry machining and the use of *Ra* as a response variable have been investigated. Once the tool, the depth of cut and the feed rate have been set, based on the previous knowledge acquired, the novelty of this work is based on a comparative study of the efficiency of different sustainable cooling systems applied to the machining of 2 different multi-material specimens and an analysis using surface roughness characterisation techniques based on the analysis of a profile and an area. This analysis makes it possible to establish two different behaviour zones in the re-drilling process, zone 1, which includes the initial 2 mm of re-drilling, and zone 2, which includes the following 4 mm. The choice of the zones was made because of the constraints of the measuring equipment and the specimen design, i.e., based on the fact that we are interested in evaluating the surface quality of the entire drilling depth, the first 2 mm cannot be measured with a contact roughness tester because it is very close to the edge, so we choose a measurement using Alicona equipment, in addition the Alicona equipment cannot measure at greater depths because of the geometry of the hole, all this determines the definition of zone 1. Zone 2 is conducted at a depth from which the measurement by contact is safe as it is far enough from the edge, and it is measured by contact as it cannot be done with the Alicona equipment. In the future, it would be interesting to redesign the specimens in a way that they can be measured using the same technology along the depth. With the aforementioned considerations in mind, it seems reasonable to establish follow-up protocols in the re-drilling repair processes in aeronautical multi-material parts that include both zones to guarantee compliance with the demanding surface tolerances required in this sector, optimising fatigue resistance and reducing the corrosion of repaired components.

A comparative experimental test was conducted on two magnesium-based multi-material specimens, *Mg-Al-Mg* and *Mg-Ti-Mg*, to investigate the influence of sustainable cooling; *cryogenic cooling*, *minimum quantity of lubricant* with eco-fluid (*MQL-Eco*), *cold compressed air (CCA)* and *dry machining* on the repair process by re-drilling. The analysis was carried out considering the values obtained in both measurement zones, in zone 1, using a measurement equipment based on an area that provides *Sa, Sz*, and the values of *Ra* and *Rz* associated with a specific profile and, in zone 2, using a Mitutoyo profilometer based on the measurement on a profile that provides the values of *Ra* and *Rz*. The study shows the influence of the different sustainable cooling tested on the surface roughness values, the factors and interactions with significant influence and their degree of influence, through the analysis of variance for each specimen combination, measurement zone or depth and chosen response variable. It is worth highlighting the differences found in the analysis depending on the type of response variable, whether it is based on a profile or an area. According to the *Ra* assessment, it is possible in specimen 1, *Mg-Al-Mg*,

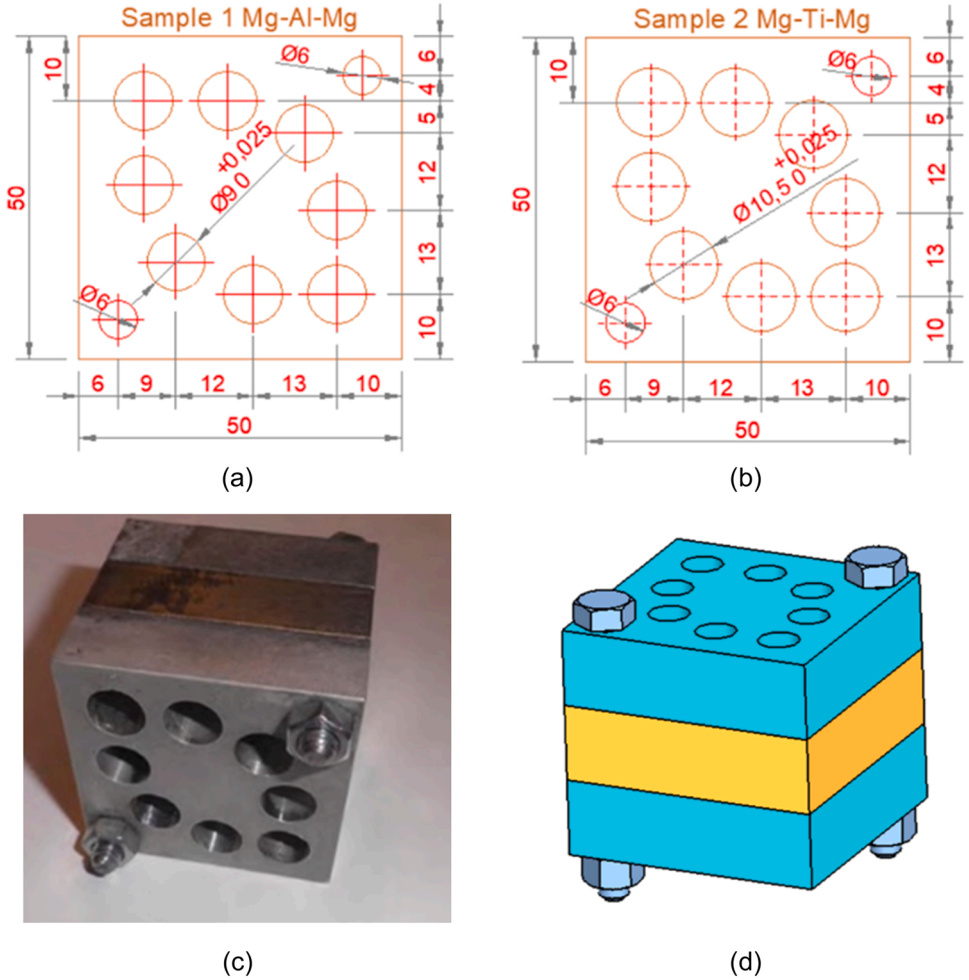

Fig. 2. Specimens: (a) Dimensions of specimens 1; (b) Dimensions of specimens 2; (c) Picture of specimen; (d) 3d representation of a specimen.

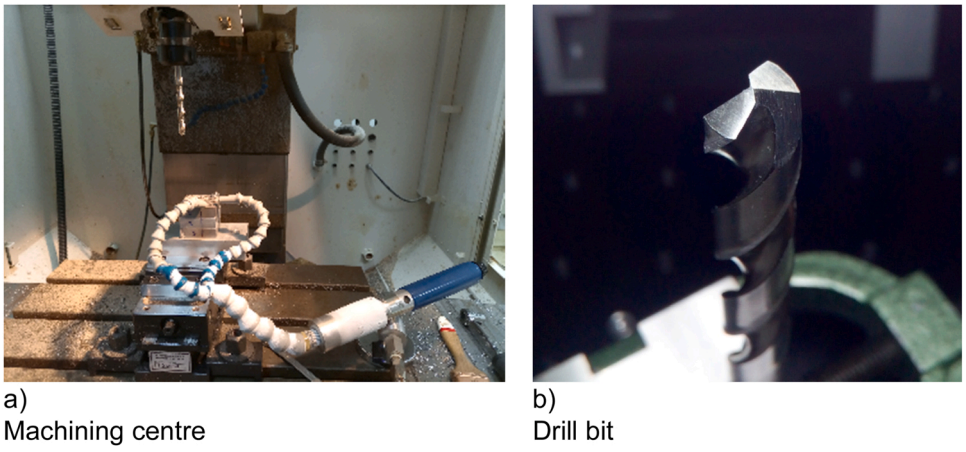

Fig. 3. Machining centre, tool: (a) Machining centre; (b) Drill bit.

to obtain all re-drilling values within the aeronautical specification [69]; using any of the sustainable cooling techniques tested. However, the process is more challenging in specimen 2, *Mg-Ti-Mg*, because titanium is a difficult material to machine and due to the difference in machinability between titanium and magnesium. The best results are obtained by *cryogenic cooling*, but there are punctual measurements slightly exceeding the aeronautical maximum tolerance, therefore it is necessary to optimise the machining parameters and particularise them for this multi-material component.

In addition, the article provides different tables that summarise and illustrate, separately and together, the factors and interactions and their degree of influence for each combination of specimen, measurement zone and response variable, and a comparison of the efficiency between the sustainable refrigeration systems tested.

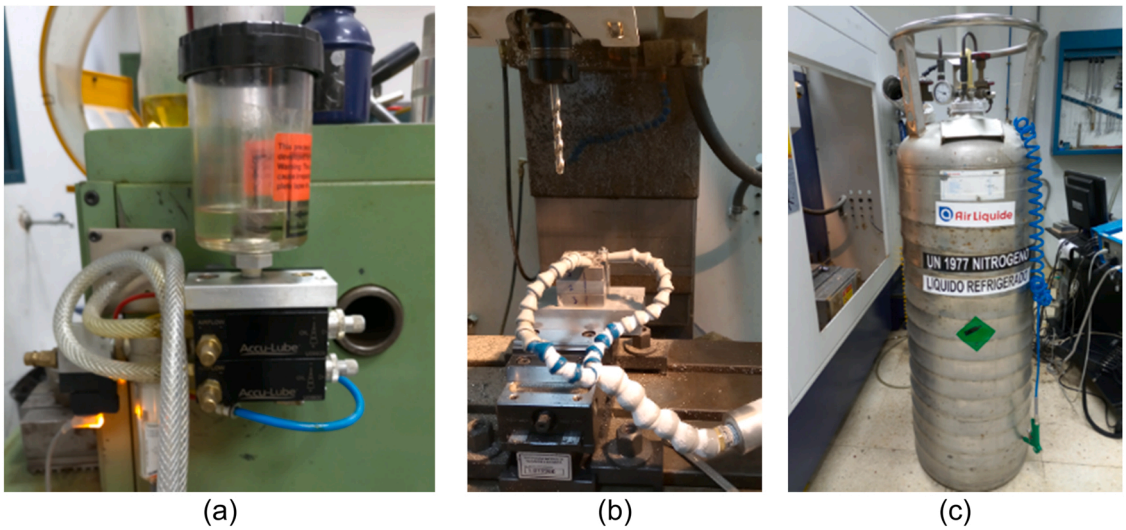

Fig. 4. Sustainable cooling equipment: (a) *MQL-Eco*; (b) *Cold Compressed Air*; (c) *Cryogenic machining.*

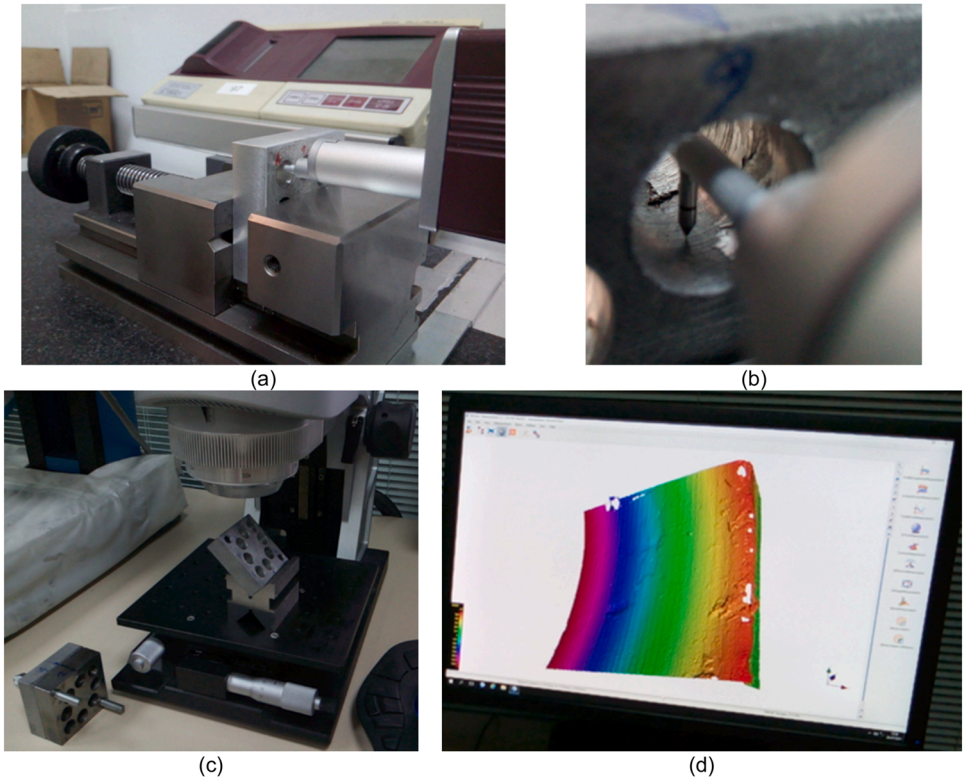

Fig. 5. Response variable measurement equipment: (a) General view of Mitutoyo roughness tester; (b) Mitutoyo roughness tester during the measurement of a drill; (c) General view of Alicona equipment; (d) Measurement made with Alicona equipment.

2. Methodology

The methodology employed starts with pre-experimental planning in which the target and scope of the research are established. Multi-material components are very trendy compounds and, with them, the aim is to obtain better global properties of the resulting material. In aeronautics and the automotive industry, the lightweighting of parts through the use of lightweight alloys and multi-materials is a topic of interest [22,67,72].

Magnesium is the lightest structural metal alloy on the planet; however, it is worth combining it with other structural alloys that enhance its mechanical properties. In addition, it is important to minimise the use of water-based cooling systems when forming because of the reactivity of water with magnesium to create flammable and potentially explosive hydrogen atmospheres [73,74]. On the other hand, it is also necessary that the sustainable process employed meets the stringent tolerances demanded by sectors such as aeronautics and the automotive industry. With this target in mind, the current study focuses on improving the understanding of the re-drilling repair process of magnesium-based multi-material parts using sustainable cooling technologies. To conduct the study, two different types of multi-material specimens were chosen; specimen 1, *Mg-Al-Mg* and specimen 2,

Table 4
Materials, tools and equipment used in the research project.

Materials and equipments	Manufacturer / supplier	Reference and relevant information	Reference
Specimen 1	Customised for experiment	3 plates of 50 × 50 × 15 Mechanical joint between plates by bolts Materials: Mg-Al-Mg Pre-drilling diameter: 9 mm	Chemical composition in . SeeFig. 2
Specimen 2	Customised for experiment	3 plates of 50x50x15 Mechanical joint between plates by bolts Materials: Mg-Ti-Mg Pre-drilling diameter: 10.5 mm	Chemical composition in Table 5. See Fig. 2
Drill bits	Güring, Brookfield, USA.	Navigator HSCO High performance twist drills Diameters 9.3 and 10.8 mm	Fig. 3b)
Machining centre +	Tongtai Machine & Tool Co, Luzhu Dist, Kaohsiung City, Taiwan.	Tongtai TMV510	Fig. 3a)
Numerical control	FANUC Iberia, Castelldefels, Barcelona, Spain.	Fanuc series OI-MC	Fig. 3a)
MQL + Eco	Accu-Lube (ITW). Georgia, USA.	Accu-Lube with frequency generator. Eco-fluid developed by Leitat Technological Centre. (Experimental stage).	Fig. 4a)
Cold compressed air system	Vortec, Cincinnati, Ohio, USA.	Compressed air working temperature of 8 °C	Fig. 4b)
Cryogenic equipment	Air Liquid, Paris, France.	Ranger 180 BP NL, Nitrogen temp. at nozzle outlet − 146.9 °C	Fig. 4c)
Roughness tester	Mitutoyo America Corporation, Aurora, IL, USA	Mitutoyo Surftest SJ 401	Fig. 5a) & b)
Surface texture	Alicona Infinitive Focus SL, Bruker Alicona	Alicona Infinitive Focus SL, optics 10x	Fig. 5c) & d)

Mg-Ti-Mg. Aluminium is a material considered easy to machine while titanium is considered difficult to machine. Therefore, the choice of materials for the test specimens allows an analysis of the machining process in magnesium-based multi-materials of different machinability and the efficiency of different types of sustainable cooling. As a preparatory step, a tool was made for two purposes: on one hand, to have a good clamping of the specimens during machining and, secondly, to provide relief at the exit of the drilling. Zero is searched for in the specimen with a sensor, obtaining greater precision. The specimen remains clamped in the tool in the same position from the start of the test, thus avoiding any deviation in the coordinates foreseen for drilling. The specimen machining programme was designed with the M 01 function (optional stop) after each drilling, in order to permit tool changes without altering the continuity of the machining programme. The different cooling systems are attached to the machining centre worktable, directly acting on the specimen and tool during the entire process.

Regarding the machining parameters, the *depth of cut, ap*, was chosen low, a single level with a value of 0.15 mm to simulate the actual conditions of a re-drilling repair operation on aeronautical and automotive parts. Since this research work is part of a larger project on which previous research has already been carried out to determine the influence of some potentially significant factors, the following factors and levels have been set: one level for the *tool, t*, which is known to have a significant influence on the process [35], one level for the *feed per rev, f (mm/rev)*; two levels for the *spindle speed, N (rev/min)*.

For the main factor on which this research is focused, four levels of sustainable refrigeration were defined: *dry machining*, *MQL-Eco* (using eco-liquid refrigerant), *cold compressed air*, and *cryogenic cooling*.

On the other hand, roughness measurements were taken in two zones, zone 1 being defined as the first 2 mm of re-drilling and zone 2 defined as the next 4 mm. These measurement zones are referenced to the entrance and exit surface of the drill hole. The choice of the zones was made because of the constraints of the measuring equipment and the specimen design.

In addition, in the re-drilling of a multi-layer multi-material compound, the position of each layer and its material, and the position at which the surface roughness measurement is taken within the re-drilled hole, are also known as potential factors of influence. The two last factors are defined as *location regarding insert, LRI*, which considers the material of the re-drilled layer and its position regarding the multi-material, and *location regarding specimen, LRS*, which analyses the roughness as a function of the position within the same layer and the direction of re-drilling. A summary of the factors and levels tested is shown in Table 1.

Surface roughness is analysed as a response variable. For this purpose, two zones are defined depending on the measuring technology to be used. *Zone 1* covers the first 2 mm with respect to the entrance and exit surfaces of the bore. *Zone 2* covers the next 4 mm, i.e., from 2 mm to 6 mm measured from the same surfaces. In zone 1, it is not possible to use a contact profile roughness tester because it is too close to the edge and errors are likely to occur. For this reason, it was decided to use optical measurements based on an area with an Alicona Infinitive Focus SL with 10x optics. In zone 2 it is not possible to measure with the Alicona equipment because it is not accessible with the design of the current multi-material specimens, so a Mitutoyo Surftest SJ 40 contact roughness tester is employed. The response variables based on surface roughness obtained from the measurements with the Alicona equipment in an area of 4 mm^2 in *zone 1* are the *arithmetic mean of the absolute values of the deviations of the surface concerning the mean plane, Sa*, and the *height of the peak to valley height of the surface, Sz*. In addition, and by defining a profile over that measured area, the *arithmetical mean deviation, Ra*, and the *maximum peak to valley height of the profile, Rz*, are obtained for that profile in *zone 1*. Alicona calculates these values considering the values measured on a 2 × 2 mm surface. The equipment obtains 4,000,000 points of the analysed surface and assigns a height to each point. This way, a surface is obtained, on which the software subsequently calculates roughness, profile, the radius of curvature, etc. by using internal algorithms. In *zone 2*, the surface roughness is measured using a roughness tester with sensor within the next 4 mm, that is, at a re-drilling depth from 2 mm to 6 mm referenced from the entry and exit surface. This area is not accessible to the Alicona equipment, but it is possible to access it with a contact profilometer roughness tester. The values employed for the study, extracted directly using the equipment software, are the *arithmetical mean deviation, Ra*, and *the maximum peak to valley height of the profile, Rz*. For each measured zone, 6 measurements are made for each drill hole and each response variable, obtaining 48 measurements for each response variable and material represented in Table 2, 96 values per response variable, and 576 total values for the 6 response variables.

The levels of the *LRI* factor that examines the influence on the surface roughness of the plate positioning within the multi-material composite are: *LRI1* (Mg1), *LRI2* (Al2/Ti2), and *LRI3* (Mg3). The levels of the *LRS* factor analysing surface roughness in relation to its positioning within each drill hole are: *LRS1* (hole entrance) and *LRS2* (hole exit). The *LRI, LRS* levels and measurement zones are shown in Fig. 1.

The next stage corresponds to the execution of the experiment. This stage includes the definition of the protocols to be used during the test and the choice of the cutting parameters. In addition, parts to be tested and drilling tools are prepared, and machining centre and sustainable cooling equipment are set up. During the execution of the experiment,

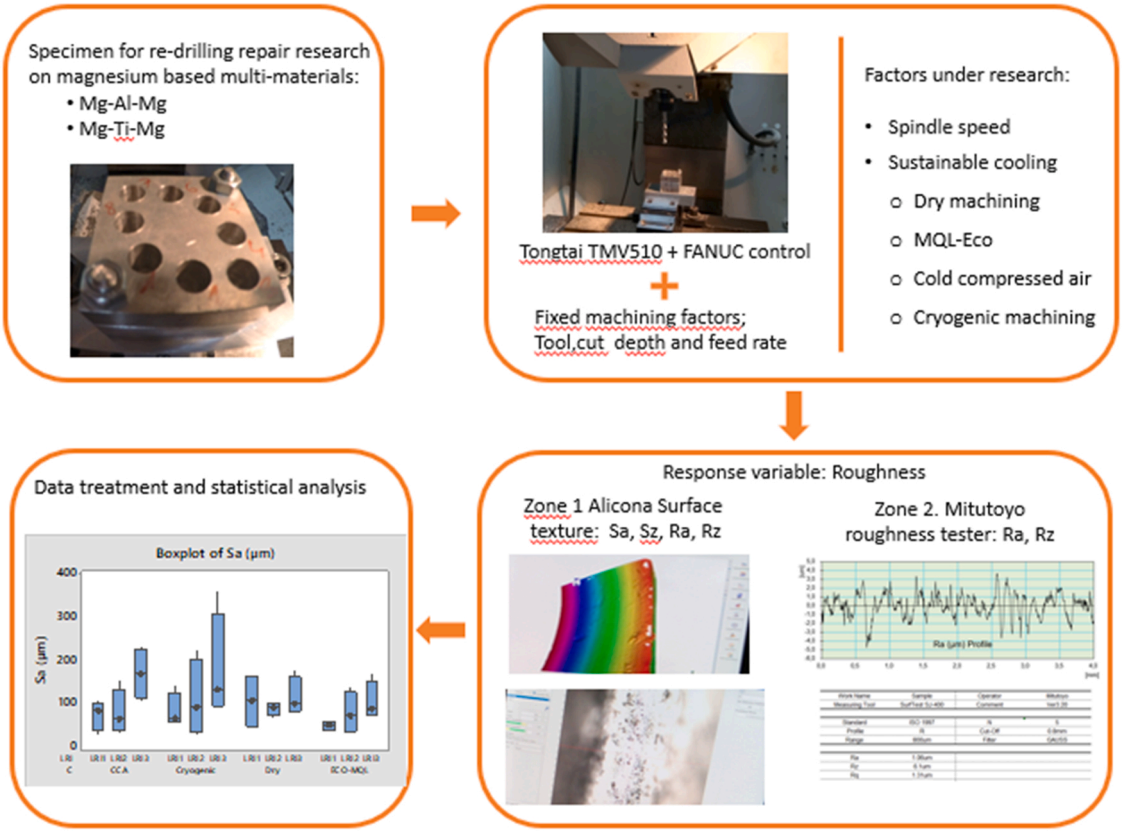

Fig. 6. Experimental setup.

Table 5
Chemical composition of the plates composing the multi-materials Mg-Al-Mg and Mg-Ti-Mg.

UNS M11917 (AZ91D)	UNS A92024 (AA2024 T351)	UNS R56400 (Ti-6Al-4 V)
Al 8.30–9.70 %	Al 90.7–94.7 %	Al 5.5–6.75 %
Cu ≤ 0.03 %	Cr ≤ 0.1 %	C ≤ 0.08 %
Fe ≤ 0.005 %	Cu 3.8–4.9 %	H ≤ 0.015 %
Mg 90 %	Fe ≤ 0.5 %	Fe ≤ 0.4 %
Mn ≥ 0.13 %	Mg 1.2–1.8 %	N ≤ 0.03 %
Ni ≤ 0.002 %	Mn 0.3–0.9 %	O ≤ 0.2 %
Si ≤ 0.1 %	Si ≤ 0.5 %	Ti 87.725–91 %
Zn 0.35–1 %	Ti ≤ 0.15 %	Zn 3.5–4.5 %
	Zn ≤ 0.25 %	

each of the re-drilling trials was filmed on video so that the process could be visualised and analysed afterwards. These videos can be visualised using the links included in Table 3 if a browser and internet connection are available. In the future, a system to fix and stabilise the camera will be integrated avoiding vibrations so that the image will be sharper and improved.

Once the machining is completed, the measurements are taken and the values of each of the response variables at the predefined measuring points are extracted. Subsequently, a statistical analysis of the data obtained is performed individually for each combination of specimen, measurement zone and response. The analysis includes a study using descriptive statistics and analysis of variance for each combination. Through these analyses, the factors and interactions with an influence on surface roughness are identified and some conclusions and recommendations are established regarding the re-drilling repair process of magnesium-based multi-material components, the sustainable cooling tested and the types of response variable employed.Fig. 2.

3. Materials, tools, equipment and specimens

The material, tools and equipment detailed in Table 4 were used to conduct the tests.

A scheme of the test setup is shown in Fig. 6. Based on the specimens of the two magnesium-based multi-material compounds, and employing four types of sustainable cooling, re-drilling repair tests are carried out with a machining centre and drills, according to a pre-established plan. As a result, Ra, Rz, Sa and Sz surface roughness values are obtained in zone 1, and Ra and Rz in zone 2. These data are statistically analysed to enhance the knowledge of the process and to select the most suitable sustainable cooling for the process.Table 5.

4. Results, analysis and discussion

The sequence of the experiment and the values obtained for each response variable are shown in Table 6 and Table 7. The only response variable for which we have the reference of the usual tolerance limits used in aeronautics is *Ra*, being 0.8 µm < *Ra* < 1.6 µm [69]. On the other hand, surface roughness below the mentioned range does not cause mechanical failure of the component, although it can add extra cost by using longer machining times and higher quality tools than those necessary. Therefore, in an optimised process, the surface quality of all the measurements of the same redrilled hole would be within the indicated range. However, values above the tolerance range do cause possible mechanical failures because of fatigue, and thus they are not acceptable in any case.

In a preliminary analysis, the data is presented in the tables below and the values obtained are compared using the colour scales defined in Fig. 7, using green for the lowest roughness values and red for the highest roughness values. The colour scale is particularised for each table. The analysis permits the values obtained to be compared in a simple and very visual way using the colour scale and, in addition, the

Table 6
Mg-Al-Mg. Values obtained for specimen 1 regarding Ra, Rz, Sa and Sz in zone 1, and Ra and Rz in zone 2.

					Zone 1				*Zone 2*	
Test	*C*	*N*	*LRI*	*LRS*	*Ra* (μm)	*Rz* (μm)	*Sa* (μm)	*Sz* (μm)	*Ra* (μm)	*Rz* (μm)
1.1	*C1*	*N1*	*LRI1*	*LRS1*	0.58	4.30	81.95	625.20	1.15	6.70
1.1	*C1*	*N1*	*LRI1*	*LRS2*	0.49	2.97	95.92	724.50	0.73	4.80
1.1	*C1*	*N1*	*LRI2*	*LRS1*	1.28	6.55	61.70	584.00	3.29	15.90
1.1	*C1*	*N1*	*LRI2*	*LRS2*	0.62	3.80	43.30	451.00	0.48	3.80
1.1	*C1*	*N1*	*LRI3*	*LRS1*	0.59	4.25	43.00	427.90	0.66	4.40
1.1	*C1*	*N1*	*LRI3*	*LRS2*	0.66	4.36	81.80	778.40	0.86	4.70
1.2	*C1*	*N2*	*LRI1*	*LRS1*	0.61	3.99	98.90	756.70	0.71	4.70
1.2	*C1*	*N2*	*LRI1*	*LRS2*	0.58	3.47	70.90	598.30	1.11	6.70
1.2	*C1*	*N2*	*LRI2*	*LRS1*	1.82	7.55	40.00	438.70	2.44	13.50
1.2	*C1*	*N2*	*LRI2*	*LRS2*	0.97	5.26	26.90	326.30	1.04	6.50
1.2	*C1*	*N2*	*LRI3*	*LRS1*	0.97	6.51	45.50	492.50	1.33	7.70
1.2	*C1*	*N2*	*LRI3*	*LRS2*	0.89	5.78	109.70	883.70	0.93	6.00
1.3	*C2*	*N1*	*LRI1*	*LRS1*	0.84	4.79	104.40	772.20	0.93	6.10
1.3	*C2*	*N1*	*LRI1*	*LRS2*	0.49	3.13	85.58	724.40	0.20	1.90
1.3	*C2*	*N1*	*LRI2*	*LRS1*	0.60	3.59	30.50	334.40	1.27	7.00
1.3	*C2*	*N1*	*LRI2*	*LRS2*	0.59	3.70	21.40	259.20	1.29	7.40
1.3	*C2*	*N1*	*LRI3*	*LRS1*	0.63	3.53	66.30	574.60	0.42	3.00
1.3	*C2*	*N1*	*LRI3*	*LRS2*	0.46	2.84	59.40	570.00	0.40	2.80
1.4	*C2*	*N2*	*LRI1*	*LRS1*	0.43	2.37	113.20	805.70	0.52	3.10
1.4	*C2*	*N2*	*LRI1*	*LRS2*	0.72	4.00	61.50	536.00	0.67	4.30
1.4	*C2*	*N2*	*LRI2*	*LRS1*	0.73	5.07	45.10	513.60	0.80	5.50
1.4	*C2*	*N2*	*LRI2*	*LRS2*	0.98	5.90	27.70	377.00	1.14	6.70
1.4	*C2*	*N2*	*LRI3*	*LRS1*	0.66	4.48	55.60	562.80	0.71	4.50
1.4	*C2*	*N2*	*LRI3*	*LRS2*	0.40	2.70	78.60	682.60	0.51	3.10
1.5	*C3*	*N1*	*LRI1*	*LRS1*	0.69	4.19	76.60	698.40	0.83	5.20
1.5	*C3*	*N1*	*LRI1*	*LRS2*	0.76	4.67	93.40	705.60	0.51	3.80
1.5	*C3*	*N1*	*LRI2*	*LRS1*	1.37	7.43	25.40	326.80	1.18	7.30
1.5	*C3*	*N1*	*LRI2*	*LRS2*	1.95	13.20	32.00	401.40	2.43	13.40
1.5	*C3*	*N1*	*LRI3*	*LRS1*	0.74	4.36	68.80	585.10	0.46	2.90
1.5	*C3*	*N1*	*LRI3*	*LRS2*	1.03	5.60	78.90	816.70	1.00	5.40
1.6	*C3*	*N2*	*LRI1*	*LRS1*	0.72	4.19	60.70	589.30	1.01	5.90
1.6	*C3*	*N2*	*LRI1*	*LRS2*	0.57	3.43	52.90	516.30	0.84	5.50
1.6	*C3*	*N2*	*LRI2*	*LRS1*	0.61	3.58	29.50	323.90	0.62	4.70
1.6	*C3*	*N2*	*LRI2*	*LRS2*	1.10	5.61	9.00	168.80	2.14	11.00
1.6	*C3*	*N2*	*LRI3*	*LRS1*	0.67	4.04	75.80	700.70	0.87	5.60
1.6	*C3*	*N2*	*LRI3*	*LRS2*	0.76	4.14	63.10	668.90	1.91	12.50
1.7	*C4*	*N1*	*LRI1*	*LRS1*	1.18	6.24	39.30	368.00	1.12	6.40
1.7	*C4*	*N1*	*LRI1*	*LRS2*	0.68	4.41	33.80	468.00	1.02	5.90
1.7	*C4*	*N1*	*LRI2*	*LRS1*	0.61	4.14	42.50	529.80	0.71	5.30
1.7	*C4*	*N1*	*LRI2*	*LRS2*	1.86	8.88	75.30	594.50	1.87	11.10
1.7	*C4*	*N1*	*LRI3*	*LRS1*	0.75	4.40	67.50	632.30	0.73	4.80
1.7	*C4*	*N1*	*LRI3*	*LRS2*	10.97	135.29	95.60	602.80	0.41	3.30
1.8	*C4*	*N2*	*LRI1*	*LRS1*	0.97	5.39	50.60	514.60	0.61	4.60
1.8	*C4*	*N2*	*LRI1*	*LRS2*	0.61	4.41	69.60	581.70	0.44	2.70
1.8	*C4*	*N2*	*LRI2*	*LRS1*	0.93	5.80	61.00	541.30	2.06	11.10
1.8	*C4*	*N2*	*LRI2*	*LRS2*	1.02	5.15	62.20	566.40	2.27	12.10
1.8	*C4*	*N2*	*LRI3*	*LRS1*	0.65	3.95	24.90	323.90	0.50	3.30
1.8	*C4*	*N2*	*LRI3*	*LRS2*	0.67	4.12	128.40	922.10	0.55	3.50

effect of the machining parameters on test and machining depth is quantified by the value shown in each cell. This analysis is carried out in individual tables per specimen, measuring zone and chosen response variable.

Within each table, several colour scales are presented, the first one SC1, which compares the values obtained for the whole set of tests. In addition, to the right of each table the average values, the standard deviation, and the maximum and minimum values of each row are calculated using the particularised colour scales for each column from SC2 to SC6 to obtain a reference of average values per multi-material specimen, measurement zone and depth. And below the table are calculated the average value, the standard deviation, and the maximum and minimum values of each column with the particularised colour scales for each row from SC7 to SC11 to obtain a reference of values for each cooling condition and rev/min, measurement zone and type of multi-material specimen.

According to the values shown in Table 8 and Table 9 and the initial comparison made by colour mapping according to the maximum and minimum roughness, it can be seen that there is not a good correlation between the surface quality assessments made by *Ra* and *Sa* in *zone 1*. The *Ra* value shaded in blue in test 1.7 was ignored as it is an outlier far higher than the rest of the test values.

Furthermore, according to the results shown in Table 8 and Table 10, there is a good correspondence between the response variables *Ra* and *Rz* measured in *zone 1*. The value shaded in blue in test 1.7 was ignored as it is an outlier far higher than the rest of the test values.

The comparison between Table 10 and Table 11 also shows a clear difference between the evaluations according to the response variables *Rz* and *Sz*.

According to the values shown in Table 12 and Table 13, and to the visual comparison of both colour mapping as a function of the maximum and minimum roughness, it is observed a good correspondence for specimen 1 between the response variables *Ra* and *Rz* in *zone 2*. Furthermore, comparing the results in Table 8 and Table 12, it is observed that the best results of *Ra*, in both zones, are produced in *MQL-Eco* conditions. This result is confirmed in Table 10 and Table 13 for the evaluations using *Rz*.

Preliminary conclusions for the second specimen are similar, the correlation between the surface quality assessments using *Ra* and *Rz* are good within the same zone as shown in Table 14 and Table 16.

Table 7
Mg-Ti-Mg. Values obtained for specimen 2 regarding Ra, Rz, Sa and Sz in zone 1, and Ra and Rz in zone 2.

					Zone 1				*Zone 2*	
Test	*C*	*N*	*LRI*	*LRS*	*Ra* (μm)	*Rz* (μm)	*Sa* (μm)	*Sz* (μm)	*Ra* (μm)	*Rz* (μm)
2.1	*C1*	*N1*	*LRI1*	*LRS1*	2.11	11.93	164.90	1456.00	1.96	14.70
2.1	*C1*	*N1*	*LRI1*	*LRS2*	1.89	10.00	159.10	1358.00	1.98	12.70
2.1	*C1*	*N1*	*LRI2*	*LRS1*	1.72	9.67	94.20	719.10	2.07	11.60
2.1	*C1*	*N1*	*LRI2*	*LRS2*	2.01	9.50	92.00	811.70	3.38	18.90
2.1	*C1*	*N1*	*LRI3*	*LRS1*	2.63	13.37	108.70	707.80	5.30	28.80
2.1	*C1*	*N1*	*LRI3*	*LRS2*	1.87	11.04	181.10	1314.00	15.40	75.40
2.2	*C1*	*N2*	*LRI1*	*LRS1*	0.74	5.23	44.90	479.60	1.60	14.70
2.2	*C1*	*N2*	*LRI1*	*LRS2*	3.42	18.19	57.80	535.00	2.09	16.80
2.2	*C1*	*N2*	*LRI2*	*LRS1*	9.02	48.41	103.10	957.60	9.83	72.30
2.2	*C1*	*N2*	*LRI2*	*LRS2*	25.01	232.50	66.20	542.50	5.92	33.60
2.2	*C1*	*N2*	*LRI3*	*LRS1*	1.37	7.67	80.80	671.10	2.80	19.50
2.2	*C1*	*N2*	*LRI3*	*LRS2*	1.21	6.82	92.10	772.10	3.35	21.00
2.3	*C2*	*N1*	*LRI1*	*LRS1*	0.58	3.63	47.50	471.30	1.29	16.50
2.3	*C2*	*N1*	*LRI1*	*LRS2*	0.87	6.47	54.10	519.00	0.99	10.10
2.3	*C2*	*N1*	*LRI2*	*LRS1*	0.74	5.23	93.40	703.00	3.16	22.40
2.3	*C2*	*N1*	*LRI2*	*LRS2*	3.24	13.00	139.40	940.20	4.94	23.70
2.3	*C2*	*N1*	*LRI3*	*LRS1*	13.62	107.09	72.30	747.90	6.65	42.30
2.3	*C2*	*N1*	*LRI3*	*LRS2*	0.92	6.56	170.80	965.00	1.26	7.90
2.4	*C2*	*N2*	*LRI1*	*LRS1*	0.82	5.28	36.70	498.70	2.81	19.10
2.4	*C2*	*N2*	*LRI1*	*LRS2*	0.73	5.56	60.10	579.60	2.64	19.30
2.4	*C2*	*N2*	*LRI2*	*LRS1*	1.27	7.54	31.00	374.40	5.04	26.10
2.4	*C2*	*N2*	*LRI2*	*LRS2*	1.45	8.56	52.40	655.80	4.14	25.10
2.4	*C2*	*N2*	*LRI3*	*LRS1*	2.12	11.86	88.20	785.90	1.71	14.00
2.4	*C2*	*N2*	*LRI3*	*LRS2*	1.22	8.79	91.00	750.90	2.60	20.50
2.5	*C3*	*N1*	*LRI1*	*LRS1*	0.80	4.73	88.90	707.50	0.99	5.40
2.5	*C3*	*N1*	*LRI1*	*LRS2*	0.70	4.16	106.60	781.90	0.65	6.00
2.5	*C3*	*N1*	*LRI2*	*LRS1*	2.29	11.44	61.60	597.70	2.98	16.40
2.5	*C3*	*N1*	*LRI2*	*LRS2*	13.52	139.82	69.20	603.20	2.81	20.80
2.5	*C3*	*N1*	*LRI3*	*LRS1*	24.85	179.82	232.80	1416.00	9.06	43.50
2.5	*C3*	*N1*	*LRI3*	*LRS2*	1.54	7.81	106.90	790.50	1.89	12.50
2.6	*C3*	*N2*	*LRI1*	*LRS1*	0.70	5.07	80.10	624.60	0.58	4.50
2.6	*C3*	*N2*	*LRI1*	*LRS2*	0.74	4.79	28.20	338.90	0.22	1.50
2.6	*C3*	*N2*	*LRI2*	*LRS1*	0.93	6.42	31.90	406.50	4.11	25.30
2.6	*C3*	*N2*	*LRI2*	*LRS2*	4.24	21.99	156.10	1055.00	8.82	44.90
2.6	*C3*	*N2*	*LRI3*	*LRS1*	5.06	37.53	206.20	903.70	7.58	43.10
2.6	*C3*	*N2*	*LRI3*	*LRS2*	4.53	30.31	135.50	854.90	2.76	16.90
2.7	*C4*	*N1*	*LRI1*	*LRS1*	1.19	8.03	56.60	597.40	1.05	5.50
2.7	*C4*	*N1*	*LRI1*	*LRS2*	1.36	8.03	144.80	928.50	0.71	4.60
2.7	*C4*	*N1*	*LRI2*	*LRS1*	0.89	6.42	48.20	525.30	1.13	7.00
2.7	*C4*	*N1*	*LRI2*	*LRS2*	0.88	6.39	136.10	1180.00	2.26	12.50
2.7	*C4*	*N1*	*LRI3*	*LRS1*	1.31	6.94	112.30	639.00	1.41	7.70
2.7	*C4*	*N1*	*LRI3*	*LRS2*	0.62	3.77	360.20	1576.00	2.01	9.80
2.8	*C4*	*N2*	*LRI1*	*LRS1*	0.80	4.84	72.10	615.50	0.36	2.80
2.8	*C4*	*N2*	*LRI1*	*LRS2*	0.65	4.11	61.00	586.80	0.30	1.60
2.8	*C4*	*N2*	*LRI2*	*LRS1*	1.27	7.37	30.30	401.60	4.97	29.80
2.8	*C4*	*N2*	*LRI2*	*LRS2*	4.96	31.38	225.60	1550.00	15.45	90.80
2.8	*C4*	*N2*	*LRI3*	*LRS1*	3.61	16.37	155.40	1031.00	0.96	6.60
2.8	*C4*	*N2*	*LRI3*	*LRS2*	0.97	5.23	90.50	738.90	1.04	8.40

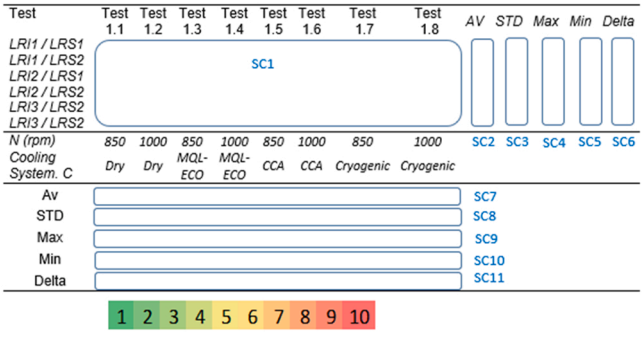

Fig. 7. Definition of the colour scales applied for the preliminary analysis.

Besides, there are differences between assessments using the same variable across different zones as shown in the analysis of *Ra* between *zones* 1 and 2 in tables Table 14 and Table 18, and in the analysis of *Rz* in tables Table 16 and Table 19, which is reasonable as it is not possible to position the profile that defines the measurement on the same line. The correlation of the assessment within *zone 1* between profile and areal variables shows very significant differences between *Ra* and *Sa* as shown in Table 14 and Table 15, and between *Rz* and *Sz* as shown in Table 16 and Table 17.

.

4.1. Mg-Al-Mg. Analysis of tests on specimen 1

Zone 1.

- Results ordered from highest to lowest roughness *Sa* and *Sz* measured within the first 2 mm of re-drilling were obtained using *CCA* < *Cryogenic* < *MQL-Eco* < *Dry*. Furthermore, a good correspondence between the response variables *Sa* and *Sz* is observed as shown in Table 9 and Table 11.
- Results ordered from highest to lowest *Ra* and *Rz* roughness measured within the first 2 mm of re-drilling were obtained using *MQL-Eco* < *CCA* < *Dry* < *Cryogenic*. Furthermore, a good

Table 8
Values obtained for specimen 1 Mg-Al-Mg regarding Ra (μm) in zone 1.

Test	Test 1.1	Test 1.2	Test 1.3	Test 1.4	Test 1.5	Test 1.6	Test 1.7	Test 1.8	*AV*	*STD*	*Max*	*Min*	*Delta*
LRI1 / LRS1	0.58	0.61	0.84	0.43	0.69	0.72	1.18	0.97	0.75	0.22	1.18	0.43	0.75
LRI1 / LRS2	0.49	0.58	0.49	0.72	0.76	0.57	0.68	0.61	0.61	0.09	0.76	0.49	0.27
LRI2 / LRS1	1.28	1.82	0.60	0.73	1.37	0.61	0.61	0.93	0.99	0.42	1.82	0.60	1.22
LRI2 / LRS2	0.62	0.97	0.59	0.98	1.95	1.10	1.86	1.02	1.14	0.48	1.95	0.59	1.36
LRI3 / LRS2	0.59	0.97	0.63	0.66	0.74	0.67	0.75	0.65	0.71	0.11	0.97	0.59	0.38
LRI3 / LRS2	0.66	0.89	0.46	0.40	1.03	0.76	10.97	0.67	0.70	0.20	1.03	0.40	0.63
N (rev/min)	*850*	*1000*	*850*	*1000*	*850*	*1000*	*850*	*1000*					
Cooling System. C	*Dry*	*Dry*	*MQL-Eco*	*MQL-Eco*	*CCA*	*CCA*	*Cryogenic*	*Cryogenic*					
Av	0.70	0.97	0.60	0.65	1.09	0.74	1.02	0.81					
STD	0.26	0.41	0.12	0.20	0.45	0.17	0.47	0.17					
Max	1.28	1.82	0.84	0.98	1.95	1.10	1.86	1.02					
Min	0.49	0.58	0.46	0.40	0.69	0.57	0.61	0.61					
Delta	0.80	1.25	0.38	0.58	1.27	0.53	1.25	0.42					

Table 9
Values obtained for specimen 1 Mg-Al-Mg regarding Sa (μm) in zone 1.

Test	Test 1.1	Test 1.2	Test 1.3	Test 1.4	Test 1.5	Test 1.6	Test 1.7	Test 1.8	*AV*	*STD*	*Max*	*Min*	*Delta*
LRI1 / LRS1	81.95	98.9	104.4	113.2	76.6	60.7	39.3	50.6	78.21	24.84	113.20	39.30	73.90
LRI1 / LRS2	95.92	70.9	85.58	61.5	93.4	52.9	33.8	69.6	70.45	19.80	95.92	33.80	62.12
LRI2 / LRS1	61.7	40	30.5	45.1	25.4	29.5	42.5	61	41.96	12.88	61.70	25.40	36.30
LRI2 / LRS2	43.3	26.9	21.4	27.7	32	9	75.3	62.2	37.23	20.56	75.30	9.00	66.30
LRI3 / LRS2	43	45.5	66.3	55.6	68.8	75.8	67.5	24.9	55.93	15.97	75.80	24.90	50.90
LRI3 / LRS2	81.8	109.7	59.4	78.6	78.9	63.1	95.6	128.4	86.94	21.79	128.40	59.40	69.00
N (rev/min)	850	1000	850	1000	850	1000	850	1000					
Cooling System. C	*Dry*	*Dry*	*MQL-Eco*	*MQL-Eco*	*CCA*	*CCA*	*Cryogenic*	*Cryogenic*					
Av	67.95	65.32	61.26	63.62	62.52	48.50	59.00	66.12					
STD	20.16	30.65	28.91	27.03	25.06	22.54	22.26	31.28					
Max	95.92	109.70	104.40	113.20	93.40	75.80	95.60	128.40					
Min	43.00	26.90	21.40	27.70	25.40	9.00	33.80	24.90					
Delta	52.92	82.80	83.00	85.50	68.00	66.80	61.80	103.50					

correspondence between the response variables *Ra* and *Rz* is observed as shown in Table 8 and Table 10.

- Tests 1.1, 1.3, 1.4, 1.6, 1.8 in Table 8 show that all Ra roughness values are within the required aeronautical specification.
- The correspondence between the area-based variables *Sa* and *Sz* and the profile-based variables *Ra* and *Rz* measured within the same *zone 1* is not good as observed from the values shown in Table 8 and Table 9, and Table 10 and Table 11 respectively.

Zone 2

- Results ordered from highest to lowest roughness *Ra* and *Rz* measured within the next 4 mm of re-drilling were obtained using *MQL* < *Cryogenic* < *CCA* < *Dry* as shown in Table 12 and Table 13.
- In tests 1.3 y 1.4 shown in Table 12, it is observed that all the measurements performed on specimen 1, *Mg-Al-Mg*, where *MQL-Eco* cooling is used, have *Ra* roughness values within the specification required in aeronautics.
- In addition, the *cryogenic cooling* conditions employed in the 1.7 tests also give good results. Although some values are above the maximum tolerance limit on the aluminium central plate, the results are very close to the limit, which means that the required tolerance could be achieved by optimising the process parameters. Also, if the average value of all the roughness measurements in the re-drilling are considered as the machining reference, the average value is within the range of the manufacturing tolerances required in aeronautics.

General

- The average of all *Ra* measurements obtained in both zones for specimen 1 is 0.93 μm.
- Assessments employing *Ra* and *Rz* as response variable in *zones 1 and 2* show a good correspondence of results between them within each zone and between different zones. According to these variables, the best results are obtained using *MQL-Eco* sustainable cooling. One part of the difference between zones is because the same measurement profile is not used since a different device is used in each zone and therefore, the definition of the measurement profile is different. In addition, there may be process differences depending on the re-drilling depth, and these are subsequently analysed through ANOVA.
- According to the profile-based data, *Ra* and *Rz*, the best compatible machining conditions for zones 1 and 2 were found for *MQL-Eco* cooling, with all values within the aeronautical tolerance and an average *Ra* value close to 0.7 μm.

Table 10
Values obtained for specimen 1 Mg-Al-Mg regarding Rz (μm) in zone 1.

Test	Test 1.1	Test 1.2	Test 1.3	Test 1.4	Test 1.5	Test 1.6	Test 1.7	Test 1.8	*AV*	*STD*	*Max*	*Min*	*Delta*
LRI1 / LRS1	4.30	3.99	4.79	2.37	4.19	4.19	6.24	5.39	4.43	1.05	6.24	2.37	3.87
LRI1 / LRS2	2.97	3.47	3.13	4.00	4.67	3.43	4.41	4.41	3.81	0.61	4.67	2.97	1.71
LRI2 / LRS1	6.55	7.55	3.59	5.07	7.43	3.58	4.14	5.80	5.46	1.52	7.55	3.58	3.97
LRI2 / LRS2	3.80	5.26	3.70	5.90	13.20	5.61	8.88	5.15	6.44	2.96	13.20	3.70	9.50
LRI3 / LRS2	4.25	6.51	3.53	4.48	4.36	4.04	4.40	3.95	4.44	0.83	6.51	3.53	2.98
LRI3 / LRS2	4.36	5.78	2.84	2.70	5.60	4.14	135.29	4.12	4.22	1.11	5.78	2.70	3.09
N (rev/min)	850	1000	850	1000	850	1000	850	1000					
Cooling System. C	*Dry*	*Dry*	*MQL-Eco*	*MQL-Eco*	*CCA*	*CCA*	*Cryogenic*	*Cryogenic*					
Av	4.37	5.43	3.60	4.09	6.58	4.17	5.61	4.80					
STD	1.09	1.40	0.61	1.24	3.16	0.71	1.80	0.68					
Max	6.55	7.55	4.79	5.90	13.20	5.61	8.88	5.80					
Min	2.97	3.47	2.84	2.37	4.19	3.43	4.14	3.95					
Delta	3.58	4.08	1.95	3.53	9.01	2.19	4.74	1.85					

Table 11
Values obtained for specimen 1 Mg-Al-Mg regarding Sz (μm) in zone 1.

Test	Test 1.1	Test 1.2	Test 1.3	Test 1.4	Test 1.5	Test 1.6	Test 1.7	Test 1.8	*AV*	*STD*	*Max*	*Min*	*Delta*
LRI1 / LRS1	625	757	772	806	698	589	368	515	641	139	806	368	438
LRI1 / LRS2	725	598	724	536	706	516	468	582	607	94	725	468	257
LRI2 / LRS1	584	439	334	514	327	324	530	541	449	101	584	324	260
LRI2 / LRS2	451	326	259	377	401	169	595	566	393	136	595	169	426
LRI3 / LRS2	428	493	575	563	585	701	632	324	537	112	701	324	377
LRI3 / LRS2	778	884	570	683	817	669	603	922	741	121	922	570	352
N (rev/min)	850	1000	850	1000	850	1000	850	1000					
Cooling System. C	*Dry*	*Dry*	*MQL-Eco*	*MQL-Eco*	*CCA*	*CCA*	*Cryogenic*	*Cryogenic*					
Av	599	583	539	580	589	495	533	575					
STD	129	190	188	135	174	190	91	177					
Max	778	884	772	806	817	701	632	922					
Min	428	326	259	377	327	169	368	324					
Delta	351	557	513	429	490	532	264	598					

- The highest surface roughness values were obtained by dry machining in zone 2 and specifically on the aluminium central plate with an *Ra* value of 3.29 μm
- The areal-based assessments *Sa* and *Sz* have a good match between their results, but a very low correlation with the profile-based results *Ra* and *Rz*. For example, the case of *CCA* test conditions 1.6 at high rev/min. The test result for these conditions shows the lowest surface roughness measured as *Sa* in *zone 1* and the second highest surface roughness measured as *Ra* in *zone 2*, as observed comparing the results in Table 9 with the values in Table 12.
- The average roughness measured as *Ra* and *Rz* depending on the *LRI* factor for both areas give similar results to previous tests measured with a contact roughness profilometer *LRI1 <LRI3 <LRI2*.
- However, the result measured in *zone 1* using the response variables *Sa* and *Sz* by Alicona equipment is entirely different. In this case, the opposite result is obtained, with the lowest roughness values in the central plate, Ti, as shown in the tables above.
- In addition, Fig. 8 shows pictures of the tool exit from the videos filmed during the machining tests. In the dry re-drilling tests 1.1 and 1.2 the highest surface roughness results are obtained, showing in the videos a small amount of smoke during drilling. For the remaining machining operations 1.3, 1.4, 1.5, 1.6, 1.7, 1.8 no significant differences were observed in the visual assessment.
- A visual inspection of the drill bit shows no deterioration of any of the tools employed during the tests on specimen 1 as observed in Fig. 10.

Fig. 9 presents the obtained values of *Ra* for each redrilled hole as a function of depth for specimen 1 Mg-Al-Mg.

Fig. 10 shows the final condition of the tool used in test 1.6 for redrilling specimen 1. This test has the highest Sz measured after redrilling with 68.27 μm.

Statistical analysis of specimen 1 data.

As observed in Fig. 11 and Fig. 12, the values of *Ra* and *Rz* have a normal distribution for zones 1 and 2, while the values of *Sa* and *Sz* do not have a normal distribution, so a logarithmic transformation is performed and the resulting values do show a normal distribution.

Fig. 13 and Fig. 14 confirm the preliminary conclusions made by the roughness colour mapping, showing how the surface roughness measured in *zones 1 and 2* by *Ra* and *Rz* obtains the lowest roughness

Table 12
Values obtained for specimen 1, Mg-Al-Mg regarding Ra (μm) in zone 2.

Test	1.1	Test 1.2	Test 1.3	Test 1.4	Test 1.5	Test 1.6	Test 1.7	Test 1.8	*AV*	*STD*	*Max*	*Min*	*Delta*
LRI1 / LRS1	1.15	0.71	0.93	0.52	0.83	1.01	1.12	0.61	0.86	0.22	1.15	0.52	0.63
LRI1 / LRS2	0.73	1.11	0.2	0.67	0.51	0.84	1.02	0.44	0.69	0.28	1.11	0.20	0.91
LRI2 / LRS1	3.29	2.44	1.27	0.8	1.18	0.62	0.71	2.06	1.55	0.90	3.29	0.62	2.67
LRI2 / LRS2	0.48	1.04	1.29	1.14	2.43	2.14	1.87	2.27	1.58	0.65	2.43	0.48	1.95
LRI3 / LRS2	0.66	1.33	0.42	0.71	0.46	0.87	0.73	0.5	0.71	0.27	1.33	0.42	0.91
LRI3 / LRS2	0.86	0.93	0.4	0.51	1	1.91	0.41	0.55	0.82	0.47	1.91	0.40	1.51
N (rev/min) Cooling System. C	850 *Dry*	1000 *Dry*	850 *MQL-Eco*	1000 *MQL-Eco*	850 *CCA*	1000 *CCA*	850 *Cryogenic*	1000 *Cryogenic*					
Av	1.20	1.26	0.75	0.73	1.07	1.23	0.98	1.07					
STD	0.96	0.56	0.43	0.21	0.66	0.58	0.46	0.78					
Max	3.29	2.44	1.29	1.14	2.43	2.14	1.87	2.27					
Min	0.48	0.71	0.20	0.51	0.46	0.62	0.41	0.44					
Delta	2.81	1.73	1.09	0.63	1.97	1.52	1.46	1.83					

Table 13
Values obtained for specimen 1. Mg-Al-Mg regarding Rz (μm) in zone 2.

Test	Test 1.1	Test 1.2	Test 1.3	Test 1.4	Test 1.5	Test 1.6	Test 1.7	Test 1.8	*AV*	*STD*	*Max*	*Min*	*Delta*
LRI1 / LRS1	6.70	4.70	6.10	3.10	5.20	5.90	6.40	4.60	5.34	1.11	6.70	3.10	3.60
LRI1 / LRS2	4.80	6.70	1.90	4.30	3.80	5.50	5.90	2.70	4.45	1.52	6.70	1.90	4.80
LRI2 / LRS1	15.90	13.50	7.00	5.50	7.30	4.70	5.30	11.10	8.79	3.92	15.90	4.70	11.20
LRI2 / LRS2	3.80	6.50	7.40	6.70	13.40	11.00	11.10	12.10	9.00	3.13	13.40	3.80	9.60
LRI3 / LRS2	4.40	7.70	3.00	4.50	2.90	5.60	4.80	3.30	4.53	1.49	7.70	2.90	4.80
LRI3 / LRS2	4.70	6.00	2.80	3.10	5.40	12.50	3.30	3.50	5.16	2.98	12.50	2.80	9.70
N (rev/min) Cooling System. C	850 *Dry*	1000 *Dry*	850 *MQL-Eco*	1000 *MQL-Eco*	850 *CCA*	1000 *CCA*	850 *Cryogenic*	1000 *Cryogenic*					
Av	6.72	7.52	4.70	4.53	6.33	7.53	6.13	6.22					
STD	4.20	2.82	2.19	1.28	3.45	3.03	2.43	3.86					
Max	15.90	13.50	7.40	6.70	13.40	12.50	11.10	12.10					
Min	3.80	4.70	1.90	3.10	2.90	4.70	3.30	2.70					
Delta	12.10	8.80	5.50	3.60	10.50	7.80	7.80	9.40					

results when *MQL-Eco* cooling is used. A large dispersion of values is also observed in the aluminium central plate, especially in *dry machining*; confirming the greater difficulty of machining aluminium compared to magnesium, and the more severe process conditions of *dry machining*. The surface roughness values of *zones 1 and 2* measured as *Ra* and *Rz* are higher for *LRI2* than for *LRI1* and *LRI3* in all refrigeration. These results are in line with previous tests. However, the conclusions for the values measured as *Sa* are different, since the central aluminium plate obtains the lowest roughness results for all the refrigeration except the cryogenic one.

No statistically significant factors or interactions are found for *Ra* and *Rz* in zone 1 as shown in Table 20 and Table 21 with all significance values above 0.05.

Table 22 presents the analysis of variance conducted on the data obtained for *Ra* in *zone 2* for specimen 1 *Mg-Al-Mg*. The analysis of variance concludes a significant influence of the factors *C*, *LRI* and the interactions of *C * LRS*, and *C*LRI * LRS* according to the percentages of influence indicated in Table 23.

Table 24 presents the analysis of variance performed on the data obtained from *Ra* in *zone 2* for specimen 1 *Mg-Al-Mg*. The analysis of variance concludes a significant influence of the factors *C*, *LRI*. and the interactions of *C * LRS*, and *C*LRI * LRS* according to the percentages of influence indicated in Table 25.

The statistically significant factors in *zone 2* are the same for the variables *Ra* and *Rz*, and the percentages of influence are similar.

Table 26 shows the analysis of variance carried out on the data obtained for *LnSa* in *zone 1* for specimen 1 *Mg-Al-Mg*. The analysis of variance concludes a significant influence of the *LRI* factor and the interactions of *LRI*C, LRI * LRS* and *C*LRS* according to the percentages indicated in Table 27.

Table 28 shows the analysis of variance performed on the data obtained for *LnSz* in *zone 1* for specimen 1 *Mg-Al-Mg*. The analysis of variance concludes a significant influence of the *LRI* factor and the interactions of *LRI*C* and *LRI * LRS* according to the percentages indicated in Table 29.

Table 30 summarises for specimen 1 *Mg-Al-Mg* the statistically significant factors and interactions identified and their percentage of influence. The table shows important differences in the significant factors and interactions of the process depending on the area analysed and the type of response variable chosen. In general, the *LRI* factor can be

Table 14
Values obtained for specimen 2 Mg-Ti-Mg regarding Ra (μm) in zone 1.

Test	Test 2.1	Test 2.2	Test 2.3	Test 2.4	Test 2.5	Test 2.6	Test 2.7	Test 2.8	*AV*	*STD*	*Max*	*Min*	*Delta*
LRI1 / LRS1	2.11	0.74	0.58	0.82	0.80	0.70	1.19	0.80	0.97	0.46	2.11	0.58	1.54
LRI1 / LRS2	1.89	3.42	0.87	0.73	0.70	0.74	1.36	0.65	1.29	0.90	3.42	0.65	2.77
LRI2 / LRS1	1.72	9.02	0.74	1.27	2.29	0.93	0.89	1.27	2.27	2.59	9.02	0.74	8.28
LRI2 / LRS2	2.01	25.01	3.24	1.45	13.52	4.24	0.88	4.96	6.91	7.79	25.01	0.88	24.13
LRI3 / LRS2	2.63	1.37	13.62	2.12	24.85	5.06	1.31	3.61	6.82	7.78	24.85	1.31	23.54
LRI3 / LRS2	1.87	1.21	0.92	1.22	1.54	4.53	0.62	0.97	1.61	1.16	4.53	0.62	3.92
N (rev/min)	850	1000	850	1000	850	1000	850	1000					
Cooling System. C	*Dry*	*Dry*	*MQL-ECO*	*MQL-ECO*	*CCA*	*CCA*	*Cryogenic*	*Cryogenic*					
Av	2.04	6.79	3.33	1.27	7.28	2.70	1.04	2.04					
STD	0.29	8.62	4.69	0.46	9.04	1.93	0.27	1.64					
Max	2.63	25.01	13.62	2.12	24.85	5.06	1.36	4.96					
Min	1.72	0.74	0.58	0.73	0.70	0.70	0.62	0.65					
Delta	0.92	24.27	13.05	1.39	24.14	4.35	0.74	4.31					

Table 15
Values obtained for specimen 2 Mg-Ti-Mg regarding Sa (μm) in zone 1.

Test	Test 2.1	Test 2.2	Test 2.3	Test 2.4	Test 2.5	Test 2.6	Test 2.7	Test 2.8	*AV*	*STD*	*Max*	*Min*	*Delta*
LRI1 / LRS1	164.9	44.9	47.5	36.7	88.9	80.1	56.6	72.1	74.0	38.4	164.9	36.7	128.2
LRI1 / LRS2	159.1	57.8	54.1	60.1	106.6	28.2	144.8	61.0	84.0	44.2	159.1	28.2	130.9
LRI2 / LRS1	94.2	103.1	93.4	31.0	61.6	31.9	48.2	30.3	61.7	29.1	103.1	30.3	72.8
LRI2 / LRS2	92.0	66.2	139.4	52.4	69.2	156.1	136.1	225.6	117.1	54.6	225.6	52.4	173.2
LRI3 / LRS2	108.7	80.8	72.3	88.2	232.8	206.2	112.3	155.4	132.1	56.2	232.8	72.3	160.5
LRI3 / LRS2	181.1	92.1	170.8	91.0	106.9	135.5	360.2	90.5	153.5	85.1	360.2	90.5	269.7
N (rev/min)	850	1000	850	1000	850	1000	850	1000					
Cooling System. C	*Dry*	*Dry*	*MQL-Eco*	*MQL-Eco*	*CCA*	*CCA*	*Cryogenic*	*Cryogenic*					
Av	133.3	74.2	96.3	59.9	111.0	106.3	143.0	105.8					
STD	36.0	20.0	45.0	23.1	57.1	65.4	103.8	65.7					
Max	181.1	103.1	170.8	91.0	232.8	206.2	360.2	225.6					
Min	92.0	44.9	47.5	31.0	61.6	28.2	48.2	30.3					
Delta	89.1	58.2	123.3	60.0	171.2	178.0	312.0	195.3					

considered the most influential factor, although it has no influence on the initial 2 mm of re-drilling.

Table 31 shows the most interesting regressions between the variables of *zone 1; Ra, Rz, Sa, Sz, LnSa* and *LnSz*, and the variables of *zone 2; Ra* and *Rz*. The correlation between variables of the same type and zone has a very high degree of explanation and significance, and the correlation decreases for variables of different zones and same type, such as *Ra* in *zone 1* and *Ra* in *zone 2*, that are measured with two different devices, the Alicona in *zone 1* and the Mitutoyo in *zone 2*, and in two different profiles, as the line of measurement cannot be positioned on the same profile. However, the degree of explanation remains high with R-Sq(adj) of 50.7 %. Similarly, the relationship between *zone 1 Rz* and *zone 2 Rz* is also high. It is interesting to highlight that the correlation between the *Ra* values of *zone 1* and *Ra* of *zone 2* is much stronger than between the *Sa* values of *zone 1* and *Ra* of *zone 1*, even though these values are obtained from the same measurement.

4.2. Mg-Ti-Mg. Analysis of tests on specimen 2

Zone 1.

- Results ordered from highest to lowest roughness Sa and Sz measured in the first 2 mm of re-drilling were obtained using *MQL-Eco* < *Dry* < *CCA* < *Cryogenic*, as shown in Table 14 and Table 16.
- Best results concerning average surface roughness in *zone 1*, measured as *Sa* and *Sz*, were obtained in test 2.4 using *MQL-Eco* cooling and 1000 rev/min.
- Highest values of surface roughness in *zone 1*, measured as *Sa* and *Sz*, were obtained by *cryogenic* cooling at low rev/min in test 2.7.
- Results ordered from highest to lowest roughness *Ra* and *Rz* measured in the first 2 mm of re-drilling were obtained using *Cryogenic* < *MQL-Eco* < *Dry* < *CCA*, as shown in Table 14 and Table 16.
- Test 2.4 shows good results when compared to the rest of the tests in *zone 1*. However, in *zone 2* this test has 5 out of 6 roughness measurements above the maximum aeronautical tolerance of 1.8 μm.
- Highest values of surface roughness in *zone 1*, measured as *Ra* and *Rz*, were obtained by *CCA* cooling at low rev/min in test 2.5, followed by *dry machining* at 1000 rev/min in test 2.2, both with values close to 4 times the maximum limit of the aeronautical tolerance used as a reference.

Table 16
Values obtained for specimen 2 Mg-Ti-Mg regarding Rz (μm) in zone 1.

Test	Test 2.1	Test 2.2	Test 2.3	Test 2.4	Test 2.5	Test 2.6	Test 2.7	Test 2.8	*AV*	*STD*	*Max*	*Min*	*Delta*
LRI1 / LRS1	11.9	5.2	3.6	5.3	4.7	5.1	8.0	4.8	6.1	2.5	11.9	3.6	8.3
LRI1 / LRS2	10.0	18.2	6.5	5.6	4.2	4.8	8.0	4.1	7.7	4.4	18.2	4.1	14.1
LRI2 / LRS1	9.7	48.4	5.2	7.5	11.4	6.4	6.4	7.4	12.8	13.6	48.4	5.2	43.2
LRI2 / LRS2	9.5	232.5	13.0	8.6	139.8	22.0	6.4	31.4	57.9	78.0	232.5	6.4	226.1
LRI3 / LRS2	13.4	7.7	107.1	11.9	179.8	37.5	6.9	16.4	47.6	58.9	179.8	6.9	172.9
LRI3 / LRS2	11.0	6.8	6.6	8.8	7.8	30.3	3.8	5.2	10.0	7.9	30.3	3.8	26.5
N (rev/min)	*850*	*1000*	*850*	*1000*	*850*	*1000*	*850*	*1000*					
Cooling System. C	*Dry*	*Dry*	*MQL-ECO*	*MQL-ECO*	*CCA*	*CCA*	*Cryogenic*	*Cryogenic*					
Av	10.9	53.1	23.7	7.9	58.0	17.7	6.6	11.5					
STD	1.4	81.6	37.4	2.2	73.0	13.1	1.4	9.8					
Max	13.4	232.5	107.1	11.9	179.8	37.5	8.0	31.4					
Min	9.5	5.2	3.6	5.3	4.2	4.8	3.8	4.1					
Delta	3.9	227.3	103.5	6.6	175.7	32.7	4.3	27.3					

Table 17
Values obtained for specimen 2 Mg-Ti-Mg regarding Sz (μm) in zone 1.

Test	Test 2.1	Test 2.2	Test 2.3	Test 2.4	Test 2.5	Test 2.6	Test 2.7	Test 2.8	*AV*	*STD*	*Max*	*Min*	*Delta*
LRI1 / LRS1	1456	480	471	499	708	625	597	616	681	303	1456	471	985
LRI1 / LRS2	1358	535	519	580	782	339	929	587	703	298	1358	339	1019
LRI2 / LRS1	719	958	703	374	598	407	525	402	586	189	958	374	583
LRI2 / LRS2	812	543	940	656	603	1055	1180	1550	917	318	1550	543	1008
LRI3 / LRS2	708	671	748	786	1416	904	639	1031	863	241	1416	639	777
LRI3 / LRS2	1314	772	965	751	791	855	1576	739	970	290	1576	739	837
N (rev/min)	850	1000	850	1000	850	1000	850	1000					
Cooling System. C	*Dry*	*Dry*	*MQL-Eco*	*MQL-Eco*	*CCA*	*CCA*	*Cryogenic*	*Cryogenic*					
Av	1061	660	724	608	816	697	908	821					
STD	319	165	188	142	279	263	373	378					
Max	1456	958	965	786	1416	1055	1576	1550					
Min	708	480	471	374	598	339	525	402					
Delta	748	478	494	412	818	716	1051	1148					

- As in specimen 1, in specimen 2 the correlation between the areal-based variables, *Sa* and *Sz*, and the profile-based variables, *Ra* and *Rz*, measured within the same zone is not good, as shown in the comparison of Table 15 and Table 17 with Table 14 and Table 16.
- In test 2.7 in Table 14, it is observed that all the *Ra* roughness values are within the required aeronautical specification. Furthermore, in test 2.4, only one of the values is out of tolerance, but close enough to optimise the process parameters to obtain all values in tolerance, for example, by lowering the spindle speed.

Zone 2

- Results ranked from highest to lowest roughness *Ra* and *Rz* measured within the next 4 mm of re-drilling were obtained using *Cryogenic* < *MQL-Eco* < *CCA* < *Dry*, as shown in Table 18 and Table 19.
- Best average roughness results *Ra* and *Rz* in *zone 2* were obtained in test 2.7 using *cryogenic cooling* and 850 rev/min as shown in Table 18 and Table 19. In addition, in this test the average drill hole value is *Ra* = 1.43 μm, lower than the upper limit of the tolerance frequently used in aeronautics. However, it has two point measurements outside the tolerance range, although close to the upper limit in the exit area of the titanium plate *LRI2 / LRS2* of 2.26 μm and in the exit of the second magnesium plate *LRI3 / LRS2* of 2.01 μm.
- This same test has the lowest roughness values measured as *Ra* in *zone 1*, and therefore they can be considered the best manufacturing conditions tested. However, it is necessary to analyse further why the worst roughness results measured as Sa are obtained in this same test 2.7.
- Test 2.8 is also conducted under cryogenically cooled conditions, but shows very high *Ra* values (15.45 μm) in *zone 2* of the titanium plate at the exit of the drill hole.
- Worst results concerning surface roughness in *zone 2*, measured as *Ra* and *Rz*, were obtained in dry machining in tests 2.1 and 2.2. However, in *zone 1*, it was produced by *cryogenic cooling*, especially at low speeds in test 2.7.

General

- The average of all *Ra* measurements in both zones for specimen 2 is 3.40 μm.
- In the same way as with specimen 1, there is a good correlation between the measured values for *Ra* and *Rz* between *zones 1 and 2*, but a clear difference between the results obtained within *zone 1*

Table 18
Values obtained for specimen 2 Mg-Ti-Mg regarding Ra (μm) in zone 2.

Test	Test 2.1	Test 2.2	Test 2.3	Test 2.4	Test 2.5	Test 2.6	Test 2.7	Test 2.8	*AV*	*STD*	*Max*	*Min*	*Delta*
LRI1 / LRS1	1.96	1.6	1.29	2.81	0.99	0.58	1.05	0.36	1.33	0.74	2.81	0.36	2.45
LRI1 / LRS2	1.98	2.09	0.99	2.64	0.65	0.22	0.71	0.3	1.20	0.85	2.64	0.22	2.42
LRI2 / LRS1	2.07	9.83	3.16	5.04	2.98	4.11	1.13	4.97	4.16	2.49	9.83	1.13	8.70
LRI2 / LRS2	3.38	5.92	4.94	4.14	2.81	8.82	2.26	15.45	5.97	4.08	15.45	2.26	13.19
LRI3 / LRS2	5.3	2.8	6.65	1.71	9.06	7.58	1.41	0.96	4.43	2.92	9.06	0.96	8.10
LRI3 / LRS2	15.4	3.35	1.26	2.6	1.89	2.76	2.01	1.04	3.79	4.45	15.40	1.04	14.36
N (rev/min)	850	1000	850	1000	850	1000	850	1000					
Cooling System. C	*Dry*	*Dry*	*MQL-Eco*	*MQL-Eco*	*CCA*	*CCA*	*Cryogenic*	*Cryogenic*					
Av	5.02	4.27	3.05	3.16	3.06	4.01	1.43	3.85					
STD	4.79	2.84	2.12	1.10	2.81	3.26	0.54	5.43					
Max	15.40	9.83	6.65	5.04	9.06	8.82	2.26	15.45					
Min	1.96	1.60	0.99	1.71	0.65	0.22	0.71	0.30					
Delta	13.44	8.23	5.66	3.33	8.41	8.60	1.55	15.15					

Table 19
Values obtained for specimen 2 Mg-Ti-Mg regarding Rz (μm) in zone 2.

Test	Test 2.1	Test 2.2	Test 2.3	Test 2.4	Test 2.5	Test 2.6	Test 2.7	Test 2.8	*AV*	*STD*	*Max*	*Min*	*Delta*
LRI1 / LRS1	14.7	14.7	16.5	19.1	5.4	4.5	5.5	2.8	10.40	6.04	19.10	2.80	16.30
LRI1 / LRS2	12.7	16.8	10.1	19.3	6	1.5	4.6	1.6	9.08	6.34	19.30	1.50	17.80
LRI2 / LRS1	11.6	72.3	22.4	26.1	16.4	25.3	7	29.8	26.36	18.81	72.30	7.00	65.30
LRI2 / LRS2	18.9	33.6	23.7	25.1	20.8	44.9	12.5	90.8	33.79	23.44	90.80	12.50	78.30
LRI3 / LRS2	28.8	19.5	42.3	14	43.5	43.1	7.7	6.6	25.69	14.87	43.50	6.60	36.90
LRI3 / LRS2	75.4	21	7.9	20.5	12.5	16.9	9.8	8.4	21.55	20.92	75.40	7.90	67.50
N (rev/min)	850	1000	850	1000	850	1000	850	1000					
Cooling System. C	*Dry*	*Dry*	*MQL-Eco*	*MQL-Eco*	*CCA*	*CCA*	*Cryogenic*	*Cryogenic*					
Av	27.02	29.65	20.48	20.68	17.43	22.70	7.85	23.33					
STD	22.38	20.00	11.34	4.04	12.86	16.98	2.65	31.60					
Max	75.40	72.30	42.30	26.10	43.50	44.90	12.50	90.80					
Min	11.60	14.70	7.90	14.00	5.40	1.50	4.60	1.60					
Delta	63.80	57.60	34.40	12.10	38.10	43.40	7.90	89.20					

between areal-based measurements, *Sa* and *Sz*, and profile-based measurements, *Ra* and *Rz*, as can be seen in Table 14, Table 15, Table 16, Table 17, Table 18 and Table 19.

- None of the conditions tested allows a machining strategy using sustainable cooling to obtain all the Ra dimensions of a re-drilling within the tolerance required in aeronautics in both areas of the drill hole.
- Test 2.7, conducted by *cryogenic cooling*, shows the best *Ra* surface roughness results, very close to the aeronautical tolerance, and is the only test on specimen 2 with an average *Ra* roughness within the aeronautical tolerance.
- Fig. 15 shows images of the tool exit filmed in the follow-up videos of the tests. Videos 2.1, 2.2, 2.3, 2.4, 2.5, 2.6 and 2.8 reveal very high tool temperature at the exit of the drill, deflagrations during machining, smoke and variation of the chip geometry during the process. These conditions are indicative of a poor final roughness result. The zone of high tool temperature is not the complete bit height or the lower zone, but the zone in contact with the LRI2 intermediate plate, about 15–20 mm from the end of the bit. Test 2.7, performed with cryogenic cooling and at lower rev/min, shows a lower and more homogeneous tool temperature, short and homogeneous chips, and no deflagration. This test obtains all Ra measurements in *zone 1* within tolerance and, in *zone 2*, values very close to the tolerance range, with average roughness less than half of the rest of the tests. However, in *zone 1*, this hole has the highest average *Sa* values, mainly due to an outlier point measurement at the exit of the second magnesium plate *LRI3/LRS2* ($Sa = 360.2$ μm).
- On subsequent visual inspection, the drill bit appears very deteriorated in all tests on specimen 2, except in test 2.7 where the best Ra roughness results were obtained in zones 1 and 2, and the worst Sa results were obtained in zone 1.
- The evaluation by *Ra* and *Rz* in *zones 1 and 2* shows an average roughness depending on *LRI* similar to previous tests, i.e., *LRI1 < LRI3 < LRI2*.
- However, the results are completely different in the evaluations conducted in *zone 1* using *Sa* and *Sz*. In this zone, *LRI1 < LRI2 < LRI3* are obtained, i.e., increasingly higher values with increasing depth.

Fig. 16 presents the evolution graphs of the roughness *Ra* as a function of the re-drilling depth for the different tests carried out on

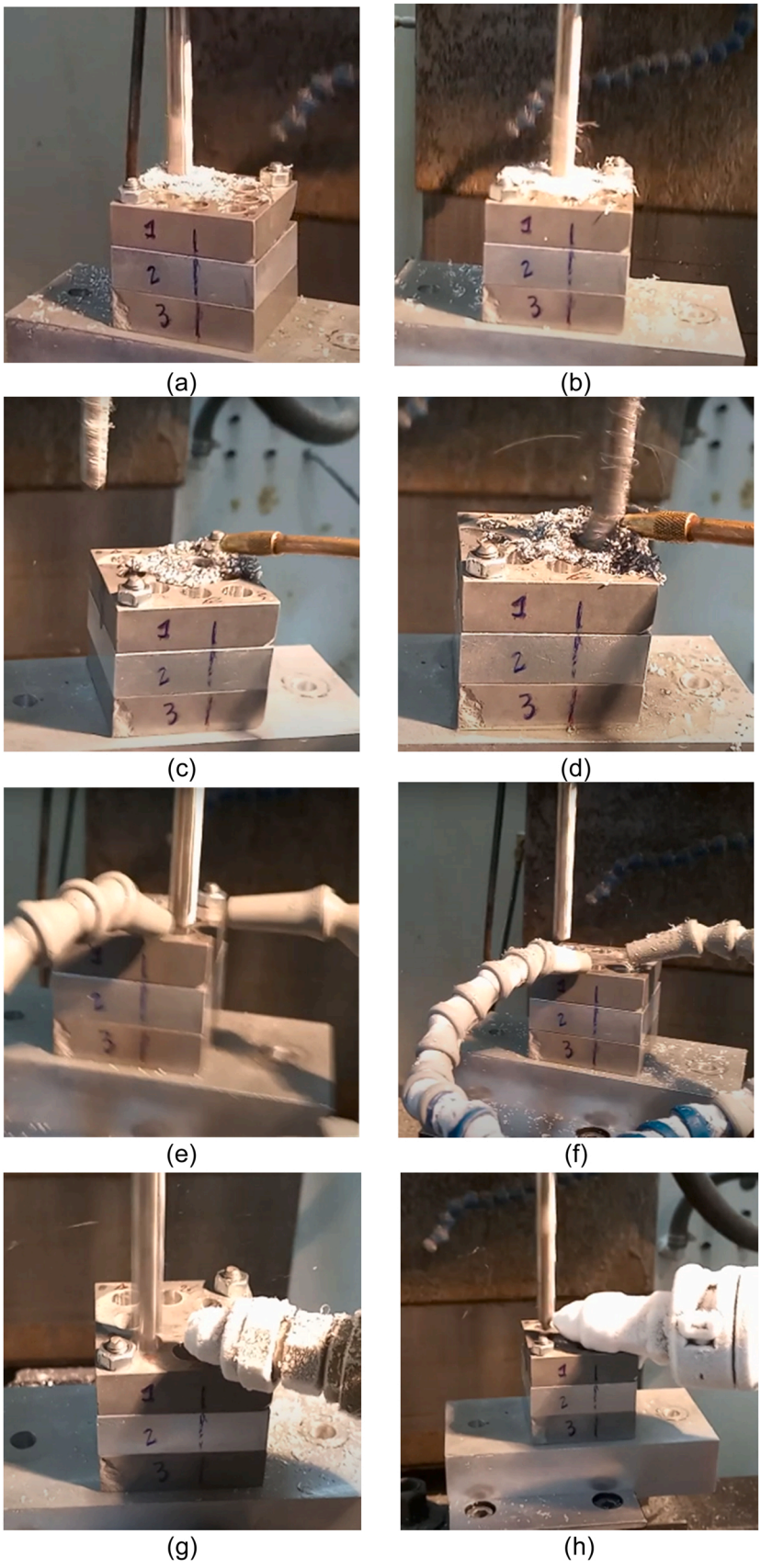

Fig. 8. *Mg-Al-Mg*. Tool exits of machining tests: (a) test 1.1; (b) test 1.2; (c) test 1.3; (d) test 1.4; (e) test 1.5; (f) test 1.6; (g) test 1.7; (h) test 1.8.

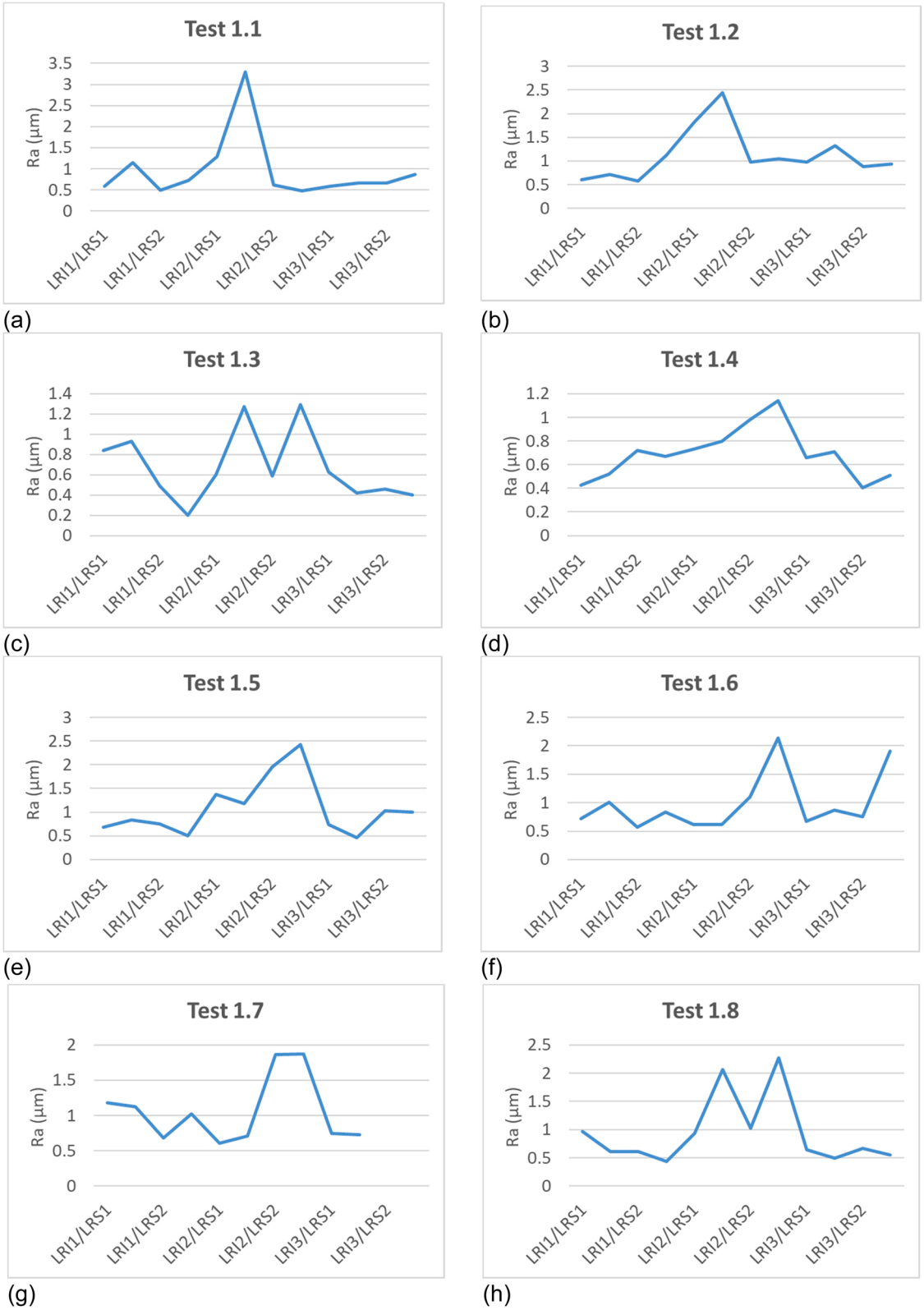

Fig. 9. Graph of the surface roughness trend as a function of the re-drilling depth measured as Ra for specimen 1. Mg-Al-Mg: (a) test 1.1; (b) test 1.2; (c) test 1.3; (d) test 1.4; (e) test 1.5; (f) test 1.6; (g) test 1.7; (h) test 1.8.

specimen 2. Fig. 17 shows the final state of the tools used in tests 2.5 and 2.7 These are the tests with the highest and lowest average *Sz* measured on both tool edges.

Statistical analysis of specimen 2 data.

Contrary to specimen 1, *Ra, Rz* values in *zones 1 and 2* and *Sa* and *Sz* values in *zone 1* follow normal distributions, so it is not necessary to carry out prior transformations before analysing the variance of the data.

Fig. 19 and Fig. 20 confirm the preliminary conclusions. It can be observed how the surface roughness measured as *Ra* and *Rz* in both

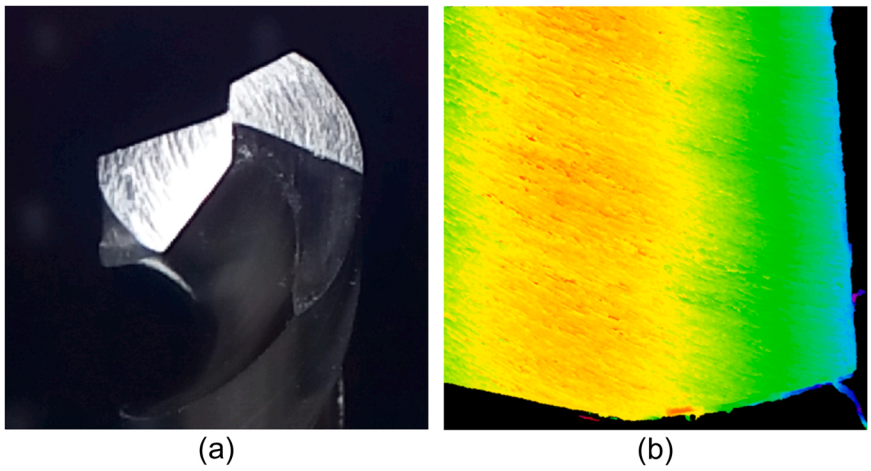

Fig. 10. Mg-Al-Mg. Condition of the tool after test 1.6 of highest Sz: (a) Conventional picture; (b) Visualization using Alicona Infinitive Focus SL, optics 10x.

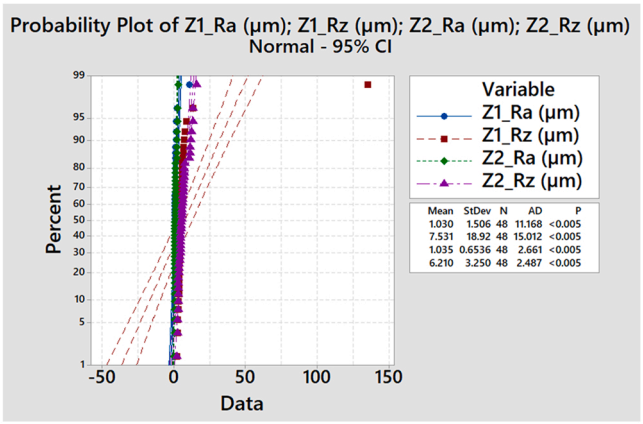

Fig. 11. Mg-Al-Mg. Plot of the probability distribution of *Ra and Rz* values in *zones 1 and 2*.

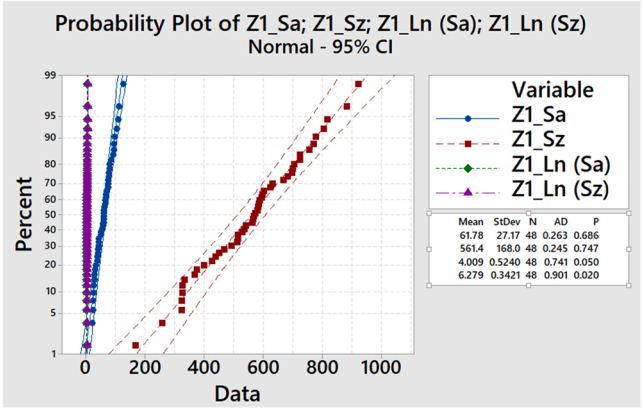

Fig. 12. Mg-Al-Mg. Probability plot of the values distribution for Sa and Sz, and the log-transform of these values, LnSa, LnSz.

zones obtains the best values for the *cryogenic cooling* conditions. Furthermore, as in the results obtained for specimen 1, similar trends are observed within the values of the same zone between the variables *Ra* and *Rz*, and with small differences between *Sa* and *Sz* within *zone 1*. Also, the results are very different when comparing roughness values profile-based, Ra and Rz, with areal-based, Sa and Sz, even when both values come from the same measurement and equipment. The results for the Ti central plates show a greater dispersion, a product of the more demanding machining process of titanium.

As shown in Table 32 and Table 33, none of the analysed factors appears as statistically significant according to the ANOVA analysis and, in both cases, the *LRI*LRS* interaction appears as significant ($p \leq 0.05$), so 100% of the influence related to the analysed factors is related to this interaction.

The analysis of variance of the surface roughness in *zone 2* measured as *Ra* for the *Mg-Ti-Mg* specimen shown in Table 34 concludes the existence of a significant influence of the *LRI* factor and the *LRI * N* interaction according to the percentages indicated in Table 35.

Similarly, the analysis of variance of the surface roughness in zone 2 measured as *Rz* for the *Mg-Ti-Mg* specimen shown in Table 36 concludes the existence of a significant influence of the *LRI* factor and the *LRI * N* interaction according to the percentages indicated in Table 37.

The analysis of variance of the surface roughness in *zone 1* measured as *Sa* for the *Mg-Ti-Mg* specimen shown in Table 38 concludes the existence of significant influence of the factors *LRI* and *N* according to the percentages indicated in Table 39.

Finally, the analysis of variance of the surface roughness in *zone 1* measured as *Sz* for the *Mg-Ti-Mg* specimen shown in Table 40 concludes that only the *N* factor is statistically significant on the *Sz* response variable in *zone 1*.

Table 41 summarises, for specimen 1, *Mg-Al-Mg*, the significant factors and interactions identified and their percentage of influence. The table shows important differences between the significant factors and interactions of the process depending on the zone studied and the type of response variable chosen.

Table 42 shows the most interesting linear regressions between the variables of *zone 1: Ra, Rz, Sa, Sz,* and the variables of zone 2: Ra and *Rz*. Similar to the results obtained with specimen 1, in specimen 2 a good correlation is observed between variables of the same type, i.e., between *Rx*, and between *Sx*, within the same zone, i.e., within *zone 1* or *zone 2*. However, the degree of explanation of the linear regressions for the same variable and different zones, e.g., *Ra* in *zone 1* and *zone 2*, is lower, although still statistically significant. Therefore, it is concluded that, although there is a relationship between the dependent and independent variable, other factors not included have a significant influence on the process. Finally, it is also remarkable that the values of *Ra* and *Sa*, and those of *Rz* and *Sz* taken in *zone 1* from the same measurement taken with the Alicona equipment do not show a significant correlation and, nevertheless, significant correlations are shown between the *Ra* and *Rz* values taken by two different equipment in two different zones, the Alicona in *zone 1* and the Mitutoyo in *zone 2*.

As a summary, and compiling the information from the previous

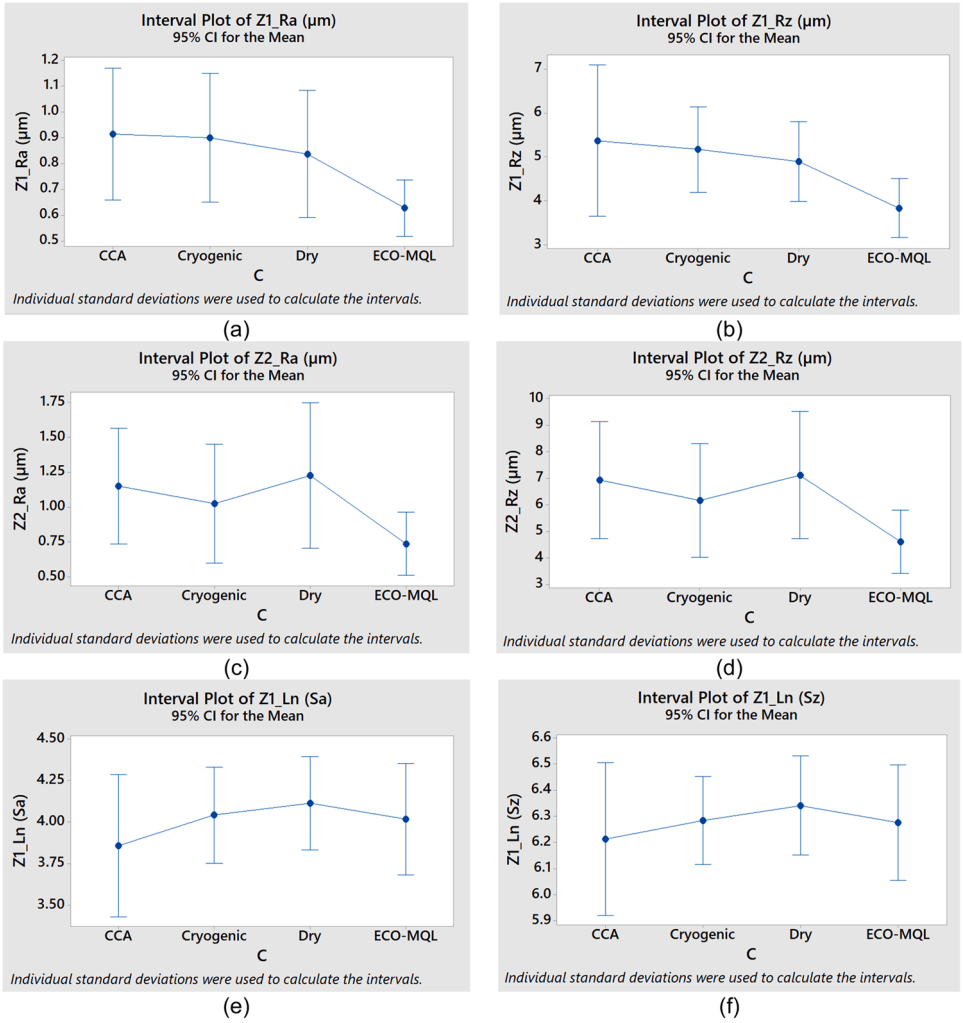

Fig. 13. Mg-Al-Mg. Interval plots: (a) Ra from zone 1; (b) Rz from zone 1; (c) Ra from zone 2 and (d) Rz from zone 2; (e) Ln Sa from zone 1; (f) LnSz from zone 1.

sections, Table 43 presents a synthesis of the surface roughness results for each combination of specimen, measurement zone and response variable analysed, showing the results according to sustainable cooling from the lowest to the highest roughness.

In addition, Table 44 summarises the significant factors and interactions identified as a function of the multi-material specimen, the zone and the response variable analysed.

4.3. Discussion

Sustainable manufacturing addresses economic, social and environmental aspects. Environmentally friendly machining seeks to minimise the consumption of cutting fluid, cutting tools and energy [49]. The main objective of this study is to investigate the influence on the re-drilling repair process of sustainable cooling; *cryogenic, minimum amount of lubricant with eco-fluid, cold compressed air* and *dry*.

The most extreme approach is the total removal of cutting fluids and thus the associated problems. However, emerging workpiece materials used especially in the aerospace industry, such as nickel, titanium or Co-Cr alloys, are extremely difficult to machine [56]. During the tests conducted on specimen 2, *Mg-Ti-Mg*, the *Ra* surface roughness values obtained by *dry machining* and *CCA* are the highest, and always higher than the values obtained by *cryogenic* and *MQL*-Eco machining, and the values obtained by *cryogenic machining* are the lowest. This is in line with the interesting review done in 2018 by García-Martínez et al. [28], in which authors conclude that *cryogenic machining* improves the surface quality of machined titanium alloy parts, although they find controversy in the studies reviewed about the possible improvement of the tool life, since if on the one hand the part and tool are cooled, on the other hand the machining forces are increased because of the increase in hardness of the titanium alloy at low temperatures.

For this reason, they find a good compromise solution using *MQL*, which reduces the amount of coolant and achieves the same, or better, surface roughness results than conventional refrigeration. In the current study, *MQL-Eco* remains a good solution, obtaining the second lowest *Ra* values in *zone 1* and *zone 2*, behind *cryogenic* refrigeration for specimen 2, and the best results in specimen1. On the other hand, other authors report an influence of the number of holes on the final roughness [20], but this could not be analysed in the current research since only 1 drill per condition was established and a new drill bit was used for each drill. According to Dixit et al., there is sufficient literature showing that the *MQL* system provides better performance than *dry machining*. In many cases, it provides better performance than the conventional coolant system [53]. In the set of trials on the 2 samples, *MQL* obtains the best global results, obtaining the best results in the sample 1, *Mg-Al-Mg*, and the second best in the sample 2, *Mg-Ti-Mg*, although the *cryogenic* option is recommended for this second sample, as it obtains values close to those required in the aeronautical sector. In *dry machining* and *MQL* tests on AA1050 aluminium specimens, Davim et al. concluded that with an appropriate choice of cutting parameters, it is possible to obtain machining results similar to the conditions of good lubrication using *MQL*, in addition tool wear is reduced and the quality of the machined

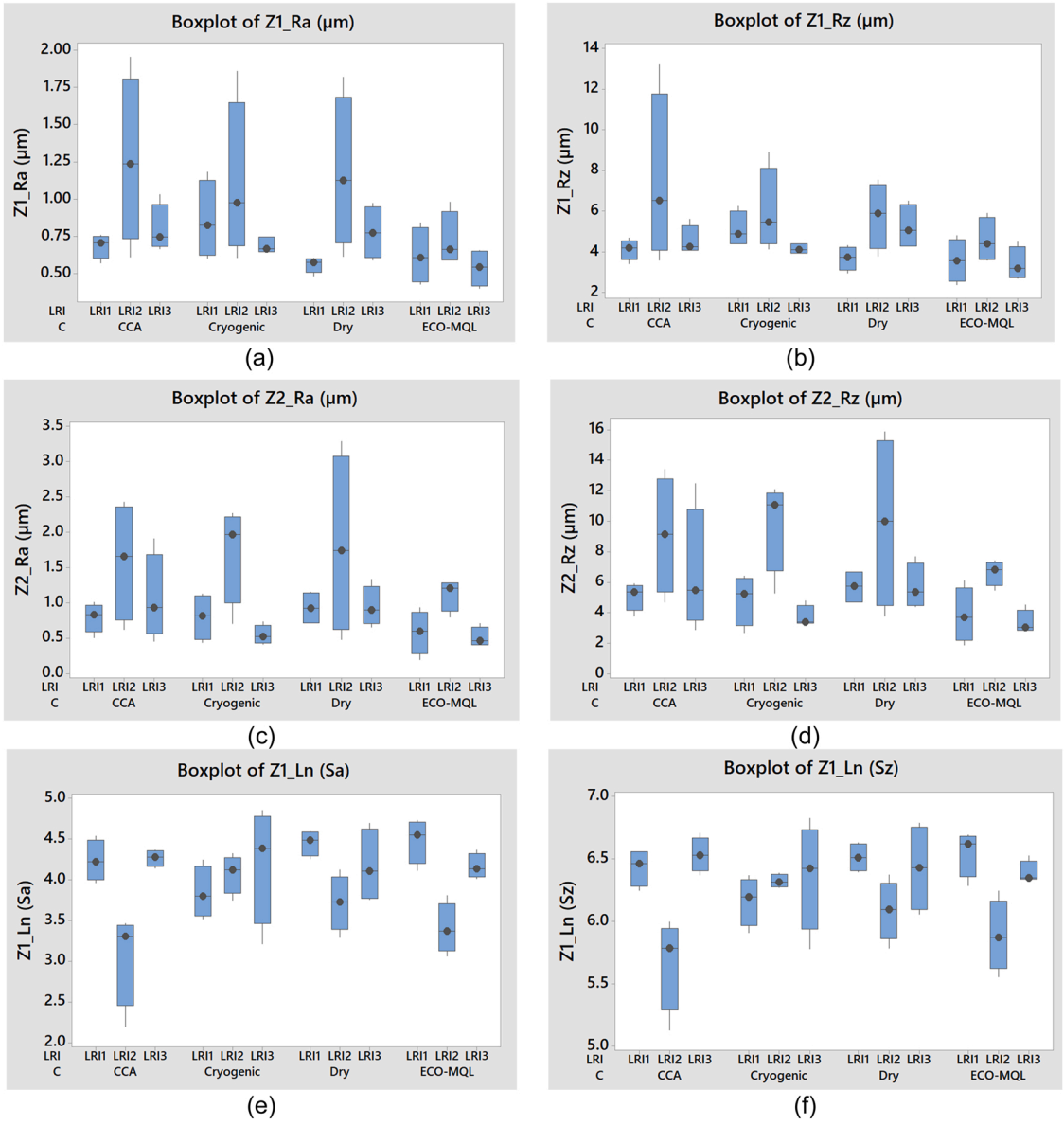

Fig. 14. *Mg-Al-Mg.* Box and whiskers graph: (a) *Ra from zone 1;* (b) *Rz from zone 1;* (c) *Ra from zone 2 and* (d) *Rz from zone 2;* (e) *Ln Sa from zone 1;* (f) *LnSz from zone 1.*

Table 20
Mg-Al-Mg. Outcome of the last iteration for the ANOVA over *Ra in zone 1.*

Tests of between-subjects effects					
Dependent variable: Z1_Ra					
Source	Sum of squares	df	Mean square	F	Sig.
Corrected Model	40,210a	15	3	1	0.263
Intercept	50.96	1.00	50.96	24.55	0.00
C	8.62	3.00	2.88	1.39	0.27
LRS	2.17	1.00	2.17	1.04	0.32
N	2.70	1.00	2.70	1.30	0.26
*C * LRS*	7.80	3.00	2.60	1.25	0.31
*C * N*	8.35	3.00	2.78	1.34	0.28
*LRS * N*	2.61	1.00	2.61	1.26	0.27
*C * LRS * N*	7.96	3.00	2.65	1.28	0.30
Error	66.43	32.00	2.08		
Total	157.61	48.00			
Corrected Total	106.64	47.00			

a R Squared = 0.377 (Adjusted R Squared = 0.085)

Table 21
Mg-Al-Mg. Outcome of the last iteration for the ANOVA over *Rz in zone 1.*

Tes[t]s of between-subjects effects					
Dependent variable: Z1_Rz					
Source	Sum of Squares	df	Mean Square	F	Sig.
Corrected Model	5695,519[a]	15	380	1	0.40
Intercept	2723	1	2723	8	0.01
C	1166	3	389	1	0.36
LRS	364	1	364	1	0.31
N	407	1	407	1	0.29
*C * LRS*	1107	3	369	1	0.38
*C * N*	1123	3	374	1	0.37
*LRS * N*	397	1	397	1	0.29
*C * LRS * N*	1132	3	377	1	0.37
Error	11,126	32	348		
Total	19,544	48			
Corrected Total	16,821	47			

[a] R Squared = 0.339 (Adjusted R Squared = 0.029)

Table 22
Mg-Al-Mg. Outcome of the last iteration for the ANOVA over *Ra in zone 2*.

Tests of between-subjects effects					
Dependent variable: *Z2_Ra*					
Source	Type III Sum of Squares	df	Mean Square	F	Sig.
Corrected Model	16.71a	23	0.73	5.17	0.00
Intercept	51.42	1	51.42	366.01	0.00
C	1.66	3	0.55	3.94	0.02
LRI	6.73	2	3.36	23.94	0.00
LRS	0.00	1	0.00	0.01	0.95
*C * LRI*	0.64	6	0.11	0.76	0.61
*C * LRS*	2.95	3	0.98	7.00	0.00
*LRI * LRS*	0.17	2	0.09	0.60	0.56
*C * LRI * LRS*	4.56	6	0.76	5.41	0.00
Error	3.37	24	0.14		
Total	71.50	48			
Corrected Total	20.08	47			

a R Squared = 0.83 (Adjusted R Squared = 0.67)

Table 23
Mg-Al-Mg. Ra-Zone 2 percentage of variability of the statistically significant effects obtained from ANOVA.

Source	Sum of squares	Variability percentage
C	1.66	10.5 %
LRI	6.73	42.3 %
*C * LRS*	2.95	18.6 %
*C * LRI * LRS*	4.56	28.7 %
Total	15.89	100 %

Table 24
Mg-Al-Mg. Outcome of the last iteration for the ANOVA over *Rz in zone 2*.

Tests of between-subjects effects					
Dependent variable: Z2_Rz					
Source	Sum of squares	df	Mean square	F	Sig.
Corrected Model	407–920a	23	17.736	4.807	0
Intercept	1851	1	1851.33	501.80	0.00
LRI	173	2	86.41	23.42	0.00
LRS	0	1	0.00	0.00	0.98
C	47	3	15.54	4.21	0.02
*LRI * LRS*	5	2	2.48	0.67	0.52
*LRI * C*	18	6	3.08	0.84	0.56
*LRS * C*	70	3	23.19	6.29	0.00
*LRI * LRS * C*	95	6	15.91	4.31	0.00
Error	89	24	3.69		
Total	2348	48			
Corrected Total	496	47			

a R Squared = 0.822 (Adjusted R Squared = 0.651)

Table 25
Mg-Al-Mg. Rz-Zone 2 percentage of variability of the statistically significant effects obtained from ANOVA.

Source	Sum of squares	Variability percentage
LRI	173	45%
C	47	12%
*LRS * C*	70	18%
*LRI * LRS * C*	95	25%
Total	384	100%

surface is improved [53].

On the other hand, there are interesting findings from researchers that deserve to be collected in this section, although the research is not explicitly focused on the scope of the current study. In 2016, Kyratsis et al. [46] analysed the relationship between the input variables of tool *diameter*, *cutting speed* and *feed rate*, and the response variables *thrust force* and *torque* when drilling a 150 mm × 150 mm × 10 mm Al7075 plate. The authors found influence of the tool *diameter* and the *feed rate* on *thrust force* and *torque*. Another aspect analysed by researchers is the vibration during the machining process, Carou et al. observed during the intermittent turning of magnesium alloy UNS M11917 that the

Table 26
Mg-Al-Mg. Outcome of the last iteration for the ANOVA over *LnSa in zone 1*.

Tests of between-subjects effects					
Dependent variable: Z1_LnSa					
Source	Sum of squares	df	Mean square	F	Sig.
Corrected Model	10,427[a]	23	0	4	0.00
Intercept	771.12	1.00	771.12	7423.12	0.00
LRI	4.69	2.00	2.35	22.60	0.00
C	0.42	3.00	0.14	1.33	0.29
LRS	0.02	1.00	0.02	0.20	0.66
*LRI * C*	2.92	6.00	0.49	4.68	0.00
*LRI * LRS*	1.11	2.00	0.55	5.34	0.01
*C * LRS*	0.89	3.00	0.30	2.84	0.06
*LRI * C * LRS*	0.39	6.00	0.06	0.62	0.71
Error	2.49	24.00	0.10		
Total	784.04	48.00			
Corrected Total	12.92	47.00			

a. R Squared = 0.807 (Adjusted R Squared =0.622)

Table 27
Mg-Al-Mg. LnSa - Zone 1 percentage of variability of the statistically significant effects obtained from ANOVA.

Source	Sum of squares	Variability percentage
LRI	4.69	49 %
*LRI * C*	2.92	30 %
*LRI * LRS*	1.11	12 %
*C * LRS*	0.89	9 %
Total	9.61	100 %

Table 28
Mg-Al-Mg. Outcome of the last iteration for the ANOVA over *LnSz in zone 1*.

Tests of between-subjects effects					
Dependent variable: Z1_LnSz					
Source	Sum of squares	df	Mean square	F	Sig.
Corrected Model	4275[a]	23	0	4	0.00
Intercept	1892.54	1.00	1892.54	36,629.82	0.00
LRI	1.98	2.00	0.99	19.18	0.00
C	0.10	3.00	0.03	0.63	0.60
LRS	0.02	1.00	0.02	0.39	0.54
*LRI * C*	1.26	6.00	0.21	4.06	0.01
*LRI * LRS*	0.56	2.00	0.28	5.38	0.01
C * LRS	0.27	3.00	0.09	1.71	0.19
LRI * C * LRS	0.10	6.00	0.02	0.31	0.92
Error	1.24	24.00	0.05		
Total	1898.06	48.00			
Corrected Total	5.51	47.00			

a. R Squared = 0.775 (Adjusted R Squared =0.560)

Table 29
Mg-Al-Mg. LnSz - Zone 1 percentage of variability of the statistically significant effects obtained from ANOVA.

Source	Sum of squares	Variability percentage
LRI	1.98	52 %
*LRI * C*	1.26	33 %
*LRI * LRS*	0.56	15 %
Total	3.79	100 %

Table 30
Mg-Al-Mg. Percentages of statistically significant influences of factors and interactions for zones 1 and 2 on response variables *Ra, Rz, LnSa* y Ln*Sz*.

	Ra		Rz		LnSa	LnSz
	Zone 1	Zone 2	Zone 1	Zone 2	Zone 1	Zone 1
LRI	–	42 %	–	45 %	49 %	52 %
C	–	10 %	–	12 %	–	–
*LRI * C*	–	–	–	–	30 %	33 %
*C * LRS*	–	19 %	–	18 %	9 %	–
*LRI * LRS*	–	–	–	–	12 %	15 %
*C * LRI * LRS*	–	29 %	–	25 %	–	–

Table 31
Mg-Al-Mg. Regression according to several independent variables, including R-Sq(adj) and P information as a function of the chosen regression relationship.

Dependent variable	Independent variable	Regression equation	R-Sq (adj)	P
Z2_Ra (μm)	Z2_Rz (μm)	Z2_Ra (μm) = -0.1989 + 0.1987 Z2_Rz (μm)	97.60 %	0.000
Z1_LnSa (μm)	Z1_LnSz (μm)	Z1_Ln (Sa) = -5.313 + 1.485 Z1_Ln (Sz)	93.80 %	0.000
Z1_Sa (μm)	Z1_Sz (μm)	Sa = - 24.21 + 0.1532 Z1_Sz	89.50 %	0.000
Z1_Ra (μm)	Z1_Rz (μm)	Z1_Ra (μm) = -0.05500 + 0.1815 Z1_Rz (μm)	86.60 %	0.000
Z2_Ra (μm)	Z1_Ra (μm)	Z2_Ra (μm) = -0.0402 + 1.330 Z1_Ra (μm)	50.70 %	0.000
Z2_Rz (μm)	Z1_Rz (μm)	Z2_Rz (μm) = 0.569 + 1.185 Z1_Rz (μm)	42.50 %	0.000
Z2_Ra (μm)	Z1_Sa (μm)	Z2_Ra (μm) = 1.494–0.007426 Z1_Sa	7.60 %	0.033
Z1_Ra (μm)	Z1_Sa (μm)	Z1_Ra (μm) = 1.047–0.003735 Z1_Sa	6.10 %	0.052
Z1_Ra (μm)	Z1_Ln (Sa)	Z1_Ra (μm) = 1.572–0.1883 Z1_Ln (Sa)	5.70 %	0.058
Z1_Rz (μm)	Z1_Sz (μm)	Z1_Rz (μm) = 6.353–0.002747 Z1_Sz	4.50 %	0.082
Z1_Rz (μm)	Z1_LnSz (μm)	Z1_Rz (μm) = 12.65–1.249 Z1_Ln (Sz)	3.50 %	0.108

measured vibration signal depends on the *MQL* flow rate and the *feed rate*. Moreover, the influence of the *MQL* system is greater when machining at the lower *feed rate*. However, this relationship is very different depending on the coolant used. While in *dry* conditions the higher the vibrations, the higher the surface roughness, the opposite is observed under *MQL* cooling. [58]. The reasons for the efficiency of *MQL* are not clear, although Lopez de Lacalle et al. [75] suggested that the air flow with oil droplets acts in three different ways; removing the heat generated during cutting, reducing the friction between chip and tool and removing the chip from the working zone.

Additionally, air is a natural resource and is available everywhere. The only processes required in the air-cooling system are compressing, drying and discharging the air at a given pressure. In most factories, compressed air is already available to perform different duties. In addition, some authors report that the performance of gas coolants, including cold compressed air, can outperform liquid coolant in some cases [60]. For example, Sarma et al. conducted a detailed comparison of *dry* and *CCA* turning in 2009 by conducting an experimental study on cast iron and steel parts and testing different tools, concluding that *CCA* always provides better machining performance than *dry machining* [61]. The results of the present work confirm that in the case of the multi-material specimen including aluminium, all the results with *CCA* are better than with *dry machining*; however, the rest of the cooling systems, *MQL-Eco* and *cryogenic*, have obtained lower roughness results. Moreover, in the case of the titanium specimen, the results in *zone 1*, the initial 2 mm of drilling, the result with *CCA* is worse than with *dry machining*. Another important factor on the roughness generation in cutting operations is the way of chip formation [68]. In fact, a chip collection was planned in the trial planning, but it was difficult for some of the tests such as *cryogenic cooling* and *CCA*, so this chip collection and analysis is postponed for a future trial, especially considering the interest of chip recycling for processes that do not contaminate the chips [55].

Furthermore, the geometry of the cutting tool has a direct impact on the tool life. This is because the geometry determines the magnitude and direction of the cutting force and its components, the sliding speed at the tool-chip interface, the distribution of the thermal energy released during machining, the temperature distribution in the cutting area, etc. [76]. For the present work, and based on the previous experience of the authors [17,35,77], a HSCO DIN 340 twist drill with 2 cutting edges and h8 diameter tolerance was selected.

Regarding the response variables employed, profile peaks rarely include the area peaks corresponding to the measured area, and similarly for profile valleys. The probability of passing over the actual highest or lowest points during the contact measurement is extremely low, and a profile that includes both is practically impossible to achieve. Another difference in values results from the properties of the filters used for processing roughness and surface profiles. As area filters work in two perpendicular directions, it is not possible to consider as equivalent the profile and area filtering results, even if the same type of filter and the same section are used [71]. This could provide a first interpretation to values such as those observed in sample 1. When using data from the same measurement with the Alicona equipment, if *Sa* and *Sz* data are analysed, *cryogenic* machining obtains the second-best results, and if *Ra* and *Rz* from zone 1 are analysed, the worst results are obtained for *cryogenic* machining. However, this explanation seems to be counter-intuitive as it seems reasonable that when all points of a surface are considered instead of just one profile to obtain the roughness, a higher value is obtained. The difference cannot correspond to a positioning error during the measurement since both values, *Sa* and *Ra*, are extracted from the analysis by the equipment's internal algorithms on the same data set belonging to the same measurement. It would be interesting to conduct further trials to better understand the difference between these measures.

5. Conclusions

A comparative experimental test was conducted on two magnesium-based multi-material specimens, *Mg-Al-Mg* and *Mg-Ti-Mg*. The main objective of the study is to investigate the influence of sustainable *cryogenic, MQL-Eco, cold compressed air* and *dry cooling* on the re-drilling repair process in magnesium-based multi-materials. The selected response variable is the surface roughness measured as *Ra, Rz, Sa* and *Sz* in *zone 1*, i.e., in the first 2 mm of re-drilling with respect to the entrance and exit surfaces of the hole and measured as *Ra* and *Rz* in *zone 2*, i.e., in the next 4 mm of re-drilling with respect to the same surfaces.

For each multi-material specimen, an analysis of the results was carried out using different complementary analysis techniques; colour range mapping according to the maximum and minimum roughness, analysis using descriptive statistics and analysis of variance to identify the factors, their significant interactions and their degree of influence. In addition, a selection of linear regressions between response variables was performed to better understand their relationship and degree of correlation.

A visual inspection of the drill bits used shows a greater degradation of the drill bits employed with the second specimen because of the greater difficulty in machining titanium.

According to the evaluation of *Ra* in specimen 1, *Mg-Al-Mg*, it is possible to obtain all re-drilling values within the aeronautical specification using any of the sustainable cooling techniques tested. The

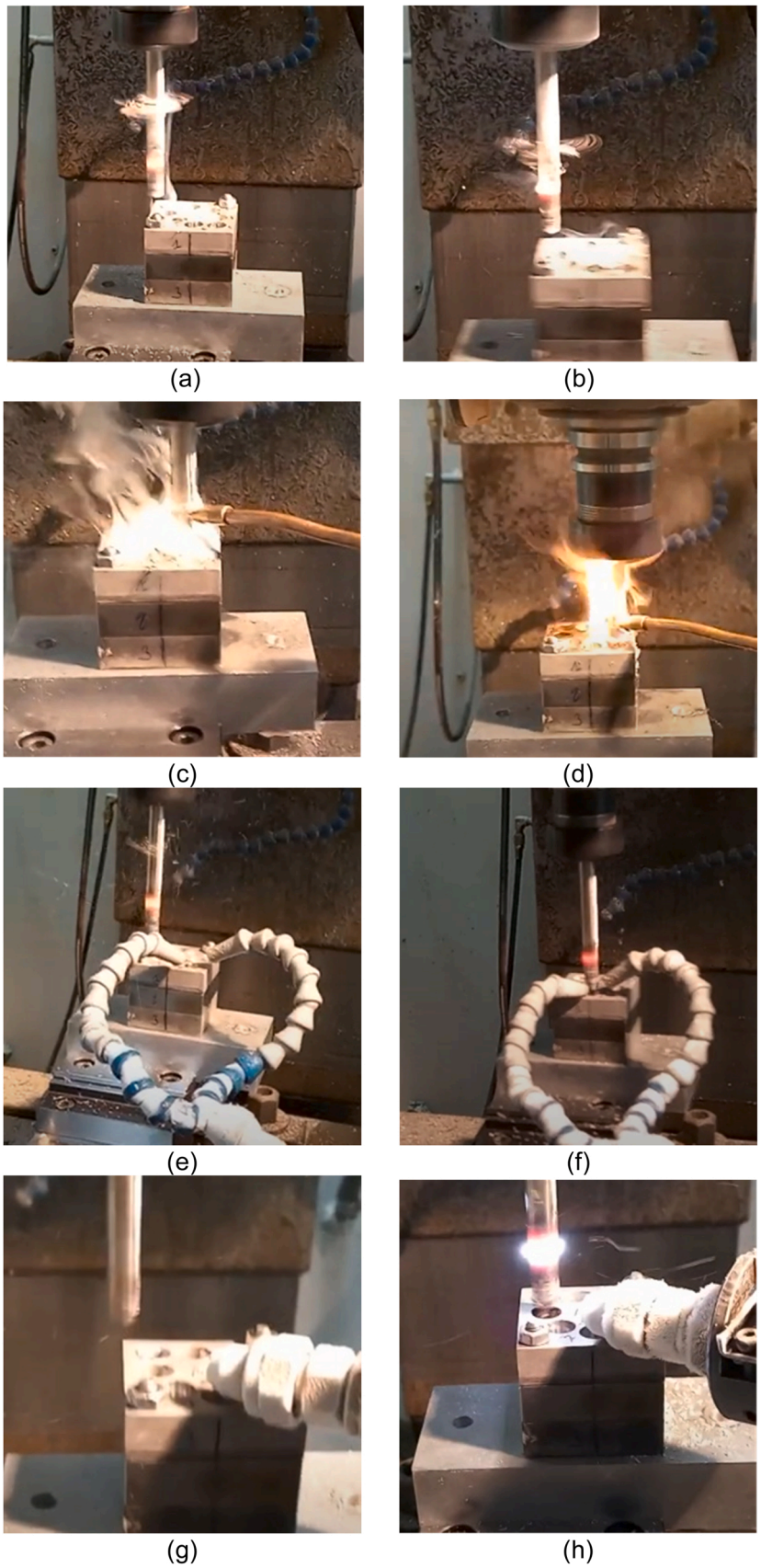

Fig. 15. *Mg-Ti-Mg.* Tool exits of machining tests; (a) test 2.1; (b) test 2.2; (c) test 2.3; (d) test 2.4; (e) test 2.5; (f) test 2.6; (g) test 2.7; (h) test 2.8.

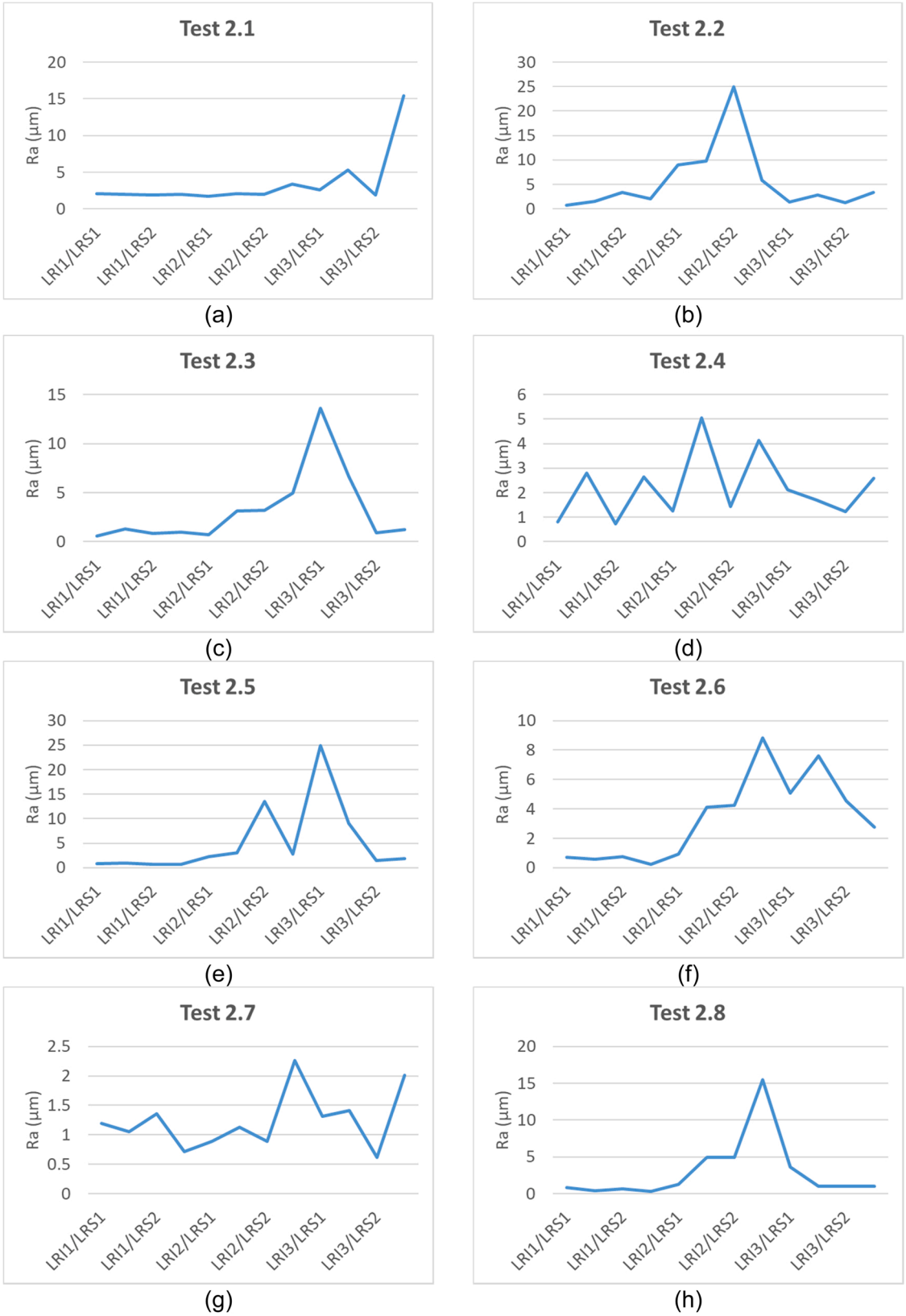

Fig. 16. Graph of the surface roughness trend as a function of the re-drilling depth measured as Ra for specimen 2, Mg-Ti-Mg: (a) test 2.1; (b) test 2.2; (c) test 2.3; (d) test 2.4; (e) test 2.5; (f) test 2.6; (g) test 2.7; (h) test 2.8.

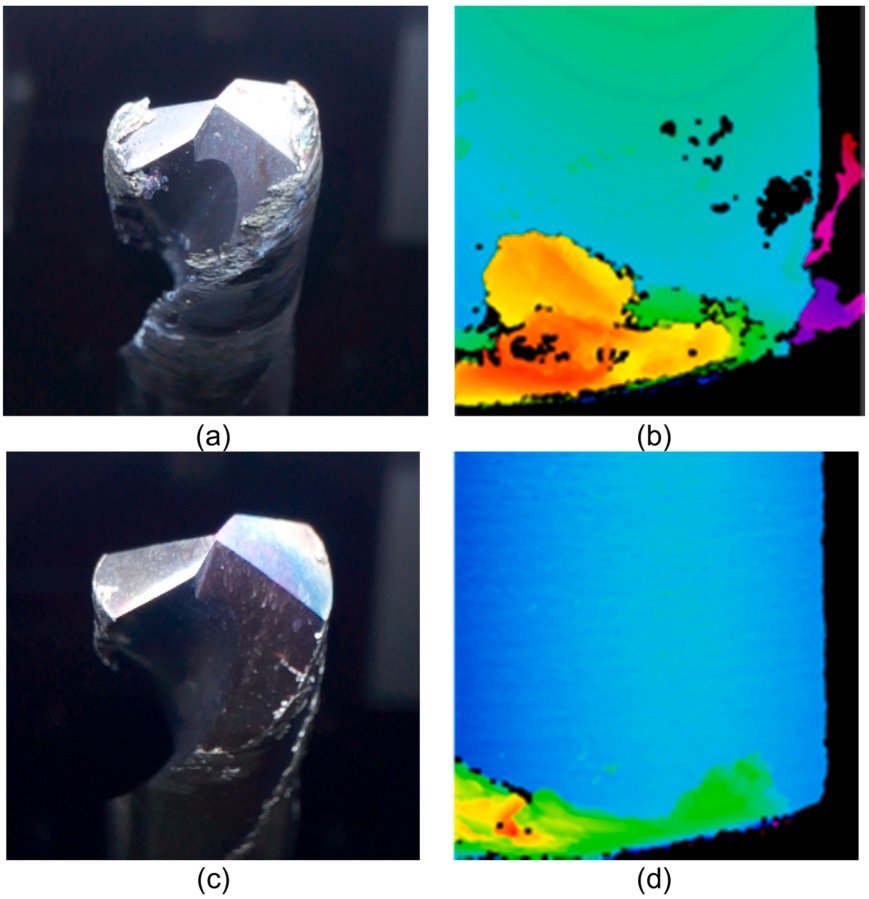

Fig. 17. Mg-Al-Mg. Condition of the tool after test 2.5 and 2.7: (a) Conventional picture after test 2.5 with highest Sz; (b) Visualization using Alicona Infinitive Focus SL, optics 10x after test 2.5with highest Sz; (c) Conventional picture after test 2.7 with lowest Sz; (d) Visualization using Alicona Infinitive Focus SL, optics 10x after test 2.7 with lowest Sz.

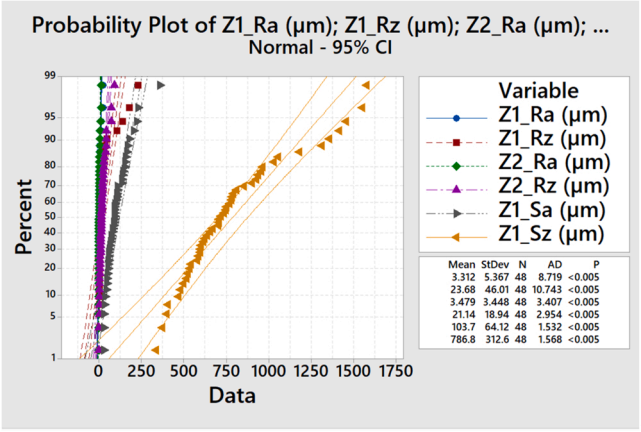

Fig. 18. Mg-Ti-Mg. Probability plot of the distribution of values of the variables *Ra* and *Rz* in *zones 1 and 2*, and of *Sa* and *Sz* in *zone 1*.

average of all *Ra* measurements in both zones for specimen 1 is 0.93 µm. However, the process is much more at the limit in specimen 2, *Mg-Ti-Mg*, because of the difficulty of machining titanium, and the average of all *Ra* measurements in both zones for specimen 2 is 3.40 µm. In addition, the difference in machinability between titanium and magnesium in specimen 2 is greater than between aluminium and magnesium in specimen 1. In the second specimen, none of the tests have all the re-drilling measurements within the tolerance range in both areas. The best results are obtained by *cryogenic cooling*, but they have punctual values slightly higher than the aeronautical upper tolerance, so it is necessary to optimise the machining parameters and particularise them for this multi-material component.

The results of the current study confirm previous literature analysed regarding the case of the multi-material specimen that includes aluminium, since all the results using CCA are better than by dry machining. However, it cannot be defined as the best sustainable option to use, since the rest of the cooling systems, MQL-Eco and cryogenic, obtained lower roughness results. Furthermore, in the case of the titanium specimen, in zone 1, the results obtained using CCA are worse than those obtained by dry machining. Furthermore, it is also confirmed in relation to the literature analysed that the use of the MQL system can contribute to improve the results of tool life or surface roughness regarding dry or wet machining, since the preliminary findings of tool inspection indicate that there is significantly less wear on the tools used in aluminium machining than in titanium machining, and that better results are obtained with MQL-Eco cooling on aluminium, and with cryogenic cooling on titanium. In the set of tests on the 2 specimens, MQL obtains the best global results, obtaining the best results in the Mg-Al-Mg specimen, and the second best in the Mg-Ti-Mg specimen, although in this second specimen the cryogenic option is recommended as it obtains values close to those required in the aeronautical sector.

The assessments, based on *Ra* and *Rz*, show a good correspondence of results within the same zone and between zones; despite the fact that between zones the measurements are made using two different devices and do not follow the same profile because an identical positioning of the measurement profile is not possible. The evaluations employing *Sa* and *Sz* have a good correspondence between their results within the

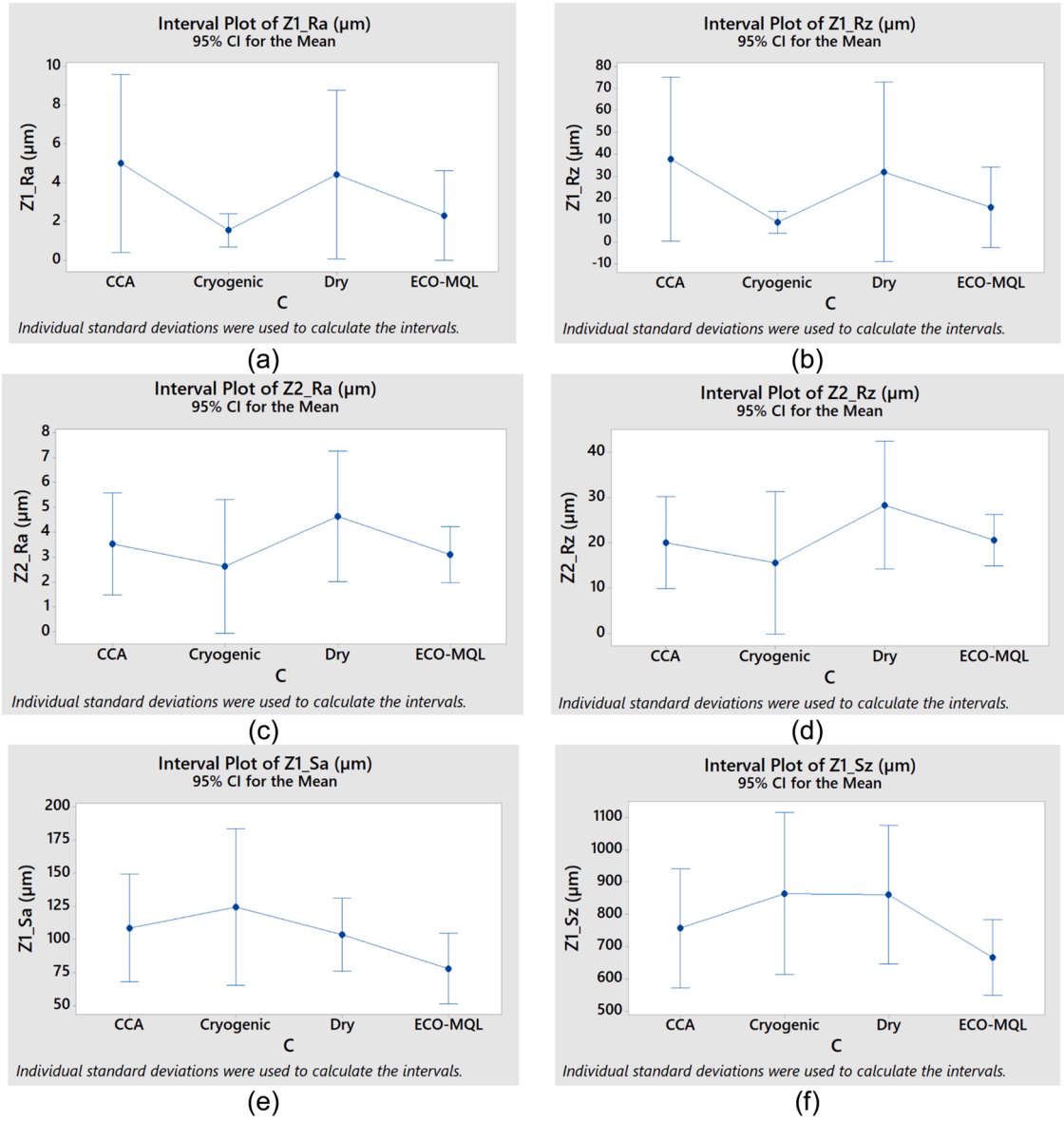

Fig. 19. Mg-Ti-Mg. Interval plots: (a) *Ra from zone 1;* (b) *Rz from zone 1;* (c) *Ra from zone 2* (d) *Rz from zone 2;* (e) *Sa from zone 1;* (f) *Sz from zone 1.*

same *zone 1*, but a very low correspondence with the results of *Ra* and *Rz* within the same *zone 1*, despite being evaluations carried out using the data collected in the same measurement with the Alicona equipment.

The statistically significant factors and interactions and their percentage of influence are different depending on: the multi-material specimen, the re-drilling zone and the response variable analysed; therefore, it is necessary to consider this when optimising the process.

Specimen 1 / Mg-Al-Mg.

General.

The best machining conditions according to *Ra*, compatible for *zones 1 and 2* were achieved using *MQL-Eco cooling*, with all values within the aeronautical reference tolerance and an average *Ra* value close to 0.7 µm. The highest surface roughness values were obtained by *dry machining* in *zone 2* and the aluminium central plate with a *Ra* value of 3.29 µm.

The average roughness measured as *Ra* and *Rz* as a function of the *LRI* factor for both zones shows similar results to previous tests measured with a contact profilometer roughness tester, *LRI1 <LRI3 <LRI2*. However, the result measured in *zone 1* using the response variables *Sa* and *Sz* is completely different, obtaining the lowest roughness values in the central Al plate.

Zone 1.

If the cooling technologies employed in the tests are ranked according to the results of the surface roughness obtained, in terms of *Ra*, from the lowest to the highest values, they appear in the following order: *MQL-Eco < CCA < Dry < Cryogenic*. The best results in terms of *Sa* are CCA < Cryogenic < MQL-Eco < Dry.

All Ra roughness values for tests 1.1, 1.3, 1.4, 1.6 and 1.8 are within the aeronautical tolerance. The correlation between areal-based variables *Sa* and *Sz* and profile-based variables *Ra* and *Rz* measured within the same area is not good, even though they are evaluations made on the basis of the same measurement over an area.

Zone 2.

If the cooling technologies employed in the tests are ranked according to the results of the surface roughness obtained, in terms of *Ra*, from the lowest to the highest values, they appear in the following order: *MQL-Eco < Cryogenic < CCA < Dry*.

The measurements conducted on specimen 1 using MQL-Eco cooling obtained all the Ra roughness values within the required aeronautical specification. In addition, the cryogenic cooling conditions used in test

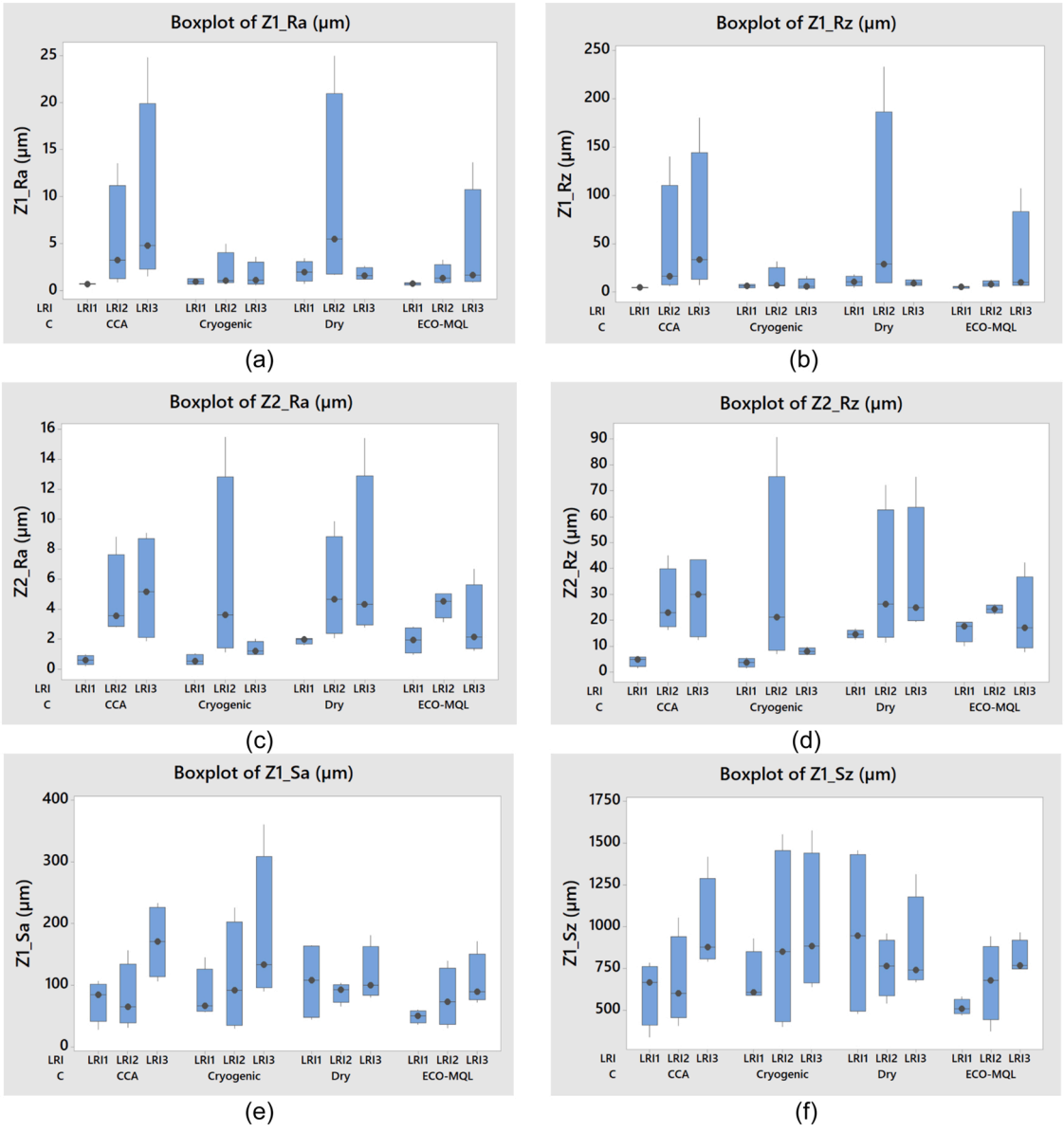

Fig. 20. *Mg-Ti-Mg.* Box and whiskers graph: (a) *Ra from zone 1;* (b) *Rz from zone 1;* (c) *Ra from zone 2* (d) *Rz from zone 2;* (e) *Sa from zone 1;*(f) *Sz from zone 1.*

Table 32
Mg-Ti-Mg. Outcome of the last iteration for the ANOVA over Ra in zone 1.

Tests of between-subjects effects					
Dependent variable: *Z1_Ra*					
Source	Sum of squares	df	Mean square	F	Sig.
Corrected Model	735.971[a]	23	32.00	1	0.30
Intercept	526.62	1.00	526.62	20.45	0.00
C	98.40	3.00	32.80	1.27	0.31
LRI	115.29	2.00	57.64	2.24	0.13
LRS	0.07	1.00	0.07	0.00	0.96
*C * LRI*	205.15	6.00	34.19	1.33	0.28
*C * LRS*	43.28	3.00	14.43	0.56	0.65
*LRI * LRS*	195.38	2.00	97.69	3.79	0.04
*C * LRI * LRS*	78.40	6.00	13.07	0.51	0.80
Error	617.93	24.00	25.75		
Total	1880.52	48.00			
Corrected Total	1353.90	47.00			

[a] . R Squared = 0.544 (Adjusted R Squared = 0.106)

Table 33
Mg-Ti-Mg. Outcome of the last iteration for the ANOVA over *Rz in zone 1.*

Tests of between-subjects effects					
Dependent variable: *Z1_Rz*					
Source	Sum of squares	df	Mean square	F	Sig.
Corrected Model	51,558.291[a]	23	2241.66	1	0.39
Intercept	26,917.06	1.00	26,917.06	13.47	0.00
C	6542.72	3.00	2180.91	1.09	0.37
LRI	7118.08	2.00	3559.04	1.78	0.19
LRS	110.69	1.00	110.69	0.06	0.82
*C * LRI*	13,296.40	6.00	2216.07	1.11	0.39
*C * LRS*	3769.99	3.00	1256.66	0.63	0.60
*LRI * LRS*	13,665.02	2.00	6832.51	3.42	0.05
*C * LRI * LRS*	7055.40	6.00	1175.90	0.59	0.74
Error	47,949.35	24.00	1997.89		
Total	126,424.70	48.00			
Corrected Total	99,507.64	47.00			

[a] . R Squared = 0.518 (Adjusted R Squared = 0.056)

Table 34
Mg-Ti-Mg. Outcome of the last iteration for the ANOVA over *Ra in zone 2*.

Tests of between-subjects effects					
Dependent variable: *Z2_Ra*					
Source	Sum of squares	df	Mean square	F	Sig.
Corrected Model	377.759[a]	23	16.42	2	0.03
Intercept	581.09	1.00	581.09	77.01	0.00
C	26.41	3.00	8.80	1.17	0.34
LRI	125.06	2.00	62.53	8.29	0.00
N	5.57	1.00	5.57	0.74	0.40
*C * LRI*	54.45	6.00	9.07	1.20	0.34
*C * N*	16.40	3.00	5.47	0.72	0.55
*LRI * N*	98.93	2.00	49.47	6.56	0.01
*C * LRI * N*	50.94	6.00	8.49	1.13	0.38
Error	181.10	24.00	7.55		
Total	1139.95	48.00			
Corrected Total	558.85	47.00			

[a]. R Squared = 0.676 (Adjusted R Squared = 0.365)

Table 35
Mg-Ti-Mg. Ra percentage of variability of the statistically significant effects obtained from ANOVA for zone 2.

Source	Sum of squares	Variability percentage
LRI	125.06	56%
LRI * N	98.9304875	44%
Total	223.99	

Table 36
Mg-Ti-Mg. Outcome of the last iteration for the ANOVA over *Rz in zone 2*.

Tests of between-subjects effects					
Dependent variable: *Z2_Rz*					
Source	Sum of squares	df	Mean square	F	Sig.
Corrected Model	11,449.253[a]	23	497.79	2	0.03
Intercept	21,458.79	1.00	21,458.79	95.16	0.00
C	1007.88	3.00	335.96	1.49	0.24
LRI	3455.93	2.00	1727.96	7.66	0.00
N	417.13	1.00	417.13	1.85	0.19
*C * LRI*	1594.07	6.00	265.68	1.18	0.35
*C * N*	406.21	3.00	135.40	0.60	0.62
*LRI * N*	2841.91	2.00	1420.95	6.30	0.01
*C * LRI * N*	1726.13	6.00	287.69	1.28	0.31
Error	5411.99	24.00	225.50		
Total	38,320.03	48.00			
Corrected Total	16,861.24	47.00			

[a]. R Squared = 0.679 (Adjusted R Squared =0.371)

Table 37
Mg-Ti-Mg. Rz percentage of variability of the statistically significant effects obtained from ANOVA for zone 2.

Source	Sum of squares	Variability percentage
LRI	3455.93	55%
LRI * N	2841.91	45%
Total	6297.83	

1.7 also show positive results.

Specimen 2 / Mg-Ti-Mg.

General.

Similar to specimen 1, there is a good correspondence between the *Ra* and *Rz* values for *zone 1*, and also between *zones 1 and 2*. However, there is a clear difference between the areal-based measurements, *Sa* and *Sz*, and the profile-based measurements *Ra* and *Rz*, within the same zone 1; both types of values were calculated from the same surface

Table 38
Mg-Ti-Mg. Outcome of the last iteration for the ANOVA over Sa in zone 1.

Tests of between-subjects effects					
Dependent variable: Z1_Sa					
Source	Sum of squares	df	Mean square	F	Sig.
Corrected Model	85,035.032[a]	11	7730.46	3	0.02
Intercept	516,446.78	1.00	516,446.78	171.81	0.00
LRI	37,515.29	2	18,757.65	6.24	0.00
N	14,162.50	1	14,162.51	4.71	0.04
LRS	10,054.34	1.00	10,054.34	3.34	0.08
*LRI * N*	5298.37	2.00	2649.18	0.88	0.42
*LRI * LRS*	4463.97	2.00	2231.98	0.74	0.48
*N * LRS*	3057.62	1.00	3057.62	1.02	0.32
*LRI * N * LRS*	10,482.95	2.00	5241.47	1.74	0.19
Error	108,211.14	36.00	3005.87		
Total	709,692.95	48.00			
Corrected Total	193,246.17	47.00			

[a]. R Squared = 0.440 (Adjusted R Squared = 0.269)

Table 39
Mg-Ti-Mg. Sa percentage of variability of the statistically significant effects obtained from ANOVA for zone 1.

Source	Sum of squares	Variability percentage
LRI	37,515.29	73 %
N	14,162.51	27 %
Total	51,677.80	

Table 40
Mg-Ti-Mg. Outcome of the last iteration for the ANOVA over Sz in zone 1.

Tests of between-subjects effects					
Dependent variable: Z1_Sz					
Source	Sum of squares	df	Mean square	F	Sig.
Corrected Model	1,671,086.52[a]	11	151,916.96	2	0.08
Intercept	29,714,918.24	1.00	29,714,918.24	366.17	0.00
LRI	431,901.38	2.00	215,950.69	2.66	0.08
LRS	283,699.50	1.00	283,699.50	3.50	0.07
N	393,385.45	1	393,385.44	4.85	0.03
*LRI * LRS*	204,441.92	2.00	102,220.96	1.26	0.30
*LRI * N*	187,354.46	2.00	93,677.23	1.15	0.33
*LRS * N*	33,591.50	1.00	33,591.50	0.41	0.52
*LRI * LRS * N*	136,712.33	2.00	68,356.16	0.84	0.44
Error	2,921,384.50	36.00	81,149.57		
Total	34,307,389.26	48.00			
Corrected Total	4,592,471.02	47.00			

[a]. R Squared = 0.364 (Adjusted R Squared = 0.170)

Table 41
Mg-Ti-Mg. Percentages of influence on response variables for significant factors and interactions in zones 1 and 2 Ra, Rz, Sa y Sz.

	Ra		Rz		Sa	Sz
	Zone 1	Zone 2	Zone 1	Zone 2	Zone 1	Zone 1
LRI		56 %		55 %	73 %	
N					27 %	100 %
*LRI * LRS*	100 %		100 %			
*LRI * N*		44 %		45 %		

measurement. On the other hand, for the second *Mg-Ti-Mg* specimen, none of the tested conditions allows defining a machining strategy using sustainable cooling that obtains all *Ra* measurements in both areas of the re-drilling within the aeronautical tolerance.

Test 2.7 by cryogenic cooling shows, in line with existing literature, the best results of surface roughness *Ra*, very close to the aeronautical tolerance, and the only test on specimen 2 with an average roughness *Ra*

Table 42
Mg-Ti-Mg. Regression according to several independent variables, including R-Sq(adj) and P information as a function of the chosen regression relationship.

Dependent variable	Independent variable	Regression equation	R-Sq (adj)	P
Z1_Ra (μm)	Z1_Rz (μm)	Z1_Ra (μm) = 0.5974 + 0.1146 Z1_Rz (μm)	96.50%	0.000
Z2_Ra (μm)	Z2_Rz (μm)	Z2_Ra (μm) = -0.2816 + 0.1779 Z2_Rz (μm)	95.40%	0.000
Z1_Sa (μm)	Z1_Sz (μm)	Z1_Sa (μm) = -42.31 + 0.1856 Z1_Sz (μm)	81.50%	0.000
Z2_Ra (μm)	Z1_Ra (μm)	Z2_Ra (μm) = 2.601 + 0.2651 Z1_Ra (μm)	15.20%	0.004
Z2_Ra (μm)	Z1_Sa (μm)	Z2_Ra (μm) = 1.434 + 0.01972 Z1_Sa (μm)	11.60%	0.010
Z2_Rz (μm)	Z1_Rz (μm)	Z2_Rz (μm) = 17.87 + 0.1384 Z1_Rz (μm)	9.40%	0.019
Z1_Ra (μm)	Z1_Sa (μm)	Z1_Ra (μm) = 1.868 + 0.01392 Z1_Sa (μm)	0.70%	0.259
Z1_Rz (μm)	Z1_Sz (μm)	Z1_Rz (μm) = 11.99 + 0.01486 Z1_Sz (μm)	0.00%	0.495

Table 43
Summary table of the most efficient sustainable cooling for each zone and specimen according to surface roughness, ranked from the lowest roughness to the highest roughness obtained.

	Mg-Al-Mg	*Mg-Ti-Mg*
Zone 1-Ra	*MQL-Eco < CCA < Dry < Cryogenic*	*Cryogenic < MQL-Eco < Dry < CCA*
Zone 2-Ra	*MQL-Eco < Cryogenic < CCA < Dry*	*Cryogenic < MQL-Eco < CCA <Dry*
Zone 1-Sa	*CCA < Cryogenic < MQL-Eco < Dry*	*MQL-Eco < Dry < CCA < Cryogenic*

Table 44
Summary table of significant factors and interactions obtained for each zone, response variable and specimen.

Zone - Variable	*Mg-Al-Mg*	*Mg-Ti-Mg*
Zone 1-Ra	*Non-significant factors and interactions*	*LRI * LRS*
Zone 1-Rz	*Non-significant factors and interactions*	*LRI * LRS*
Zone 2-Ra	*LRI / C / C*LRS / C*LRI / LRS*	*LRI / LRI * N*
Zone 2-Rz	*LRI / C / C*LRS / C*LRI*LRS*	*LRI / LRI * N*
Zone 1-Sa	*Not applicable*	*LRI / N*
Zone 1-Sz	*Not applicable*	*N*
Zone 1-LnSa	*LRI / LRI*C / LRI*LRS / C*LRS*	*Not applicable*
Zone 1-LnSz	*LRI / LRI*C / LRI*LRS*	*Not applicable*

within the aeronautical tolerance. The evaluation by *Ra* and *Rz* in *zones 1 and 2* shows an average roughness depending on *LRI* similar to previous tests, i.e., *LRI1 <LRI3 <LRI2*. However, the results are completely different in the evaluations carried out in *zone 1* using *Sa* and *Sz*. In this zone, *LRI1 <LRI2 <LRI3* are obtained, i.e., higher and higher values with increasing depth.

On further visual inspection, the drill bit appears badly degraded in all tests on specimen 2, except for test 2.7. Worst surface roughness results depend on the chosen response variable and were produced using *dry machining* for *Ra* and *Rz*, and *cryogenic cooling* for *Sa* and *Sz*.

Zone 1.

If the cooling technologies applied during the tests are ranked according to the results of the surface roughness obtained, in terms of *Ra*, from the lowest to the highest values, they appear in the following order: *Cryogenic< MQL-Eco < Dry < CCA*. The best results in terms of *Sa* are obtained with *MQL-Eco < Dry < CCA < Cryogenic*.

Test 2.4 achieves good results in *zone 1*, but negative results considering zones 1 and 2. The highest values of surface roughness in *zone 1*, measured as *Ra* and *Rz*, are obtained in test 2.5 using *CCA cooling* at 850 rev/min, followed by test 2.2 using *dry machining* at 1000 rev/min; both with values close to 4 times the maximum limit of the aeronautical tolerance used as a reference.

Zona 2.

If the cooling systems applied in the tests are ranked considering the results of the surface roughness obtained, in terms of *Ra*, from the lowest to the highest values, they appear in the following order: *Cryogenic < MQL-Eco < CCA < Dry*. The best average roughness results *Ra* and *Rz* were obtained in test 2.7 using *cryogenic cooling* and 850 rev/min. Furthermore, in this test the average hole roughness value is $Ra = 1.43$ μm, which is lower than the upper limit of the tolerance often used in aeronautics. However, it has punctual measurements in the exit area of the titanium plate *LRI2 / LRS2* of 2.26 μm and in the exit of the second magnesium plate *LRI3/LRS2* of 2.01 μm. However, this same test, evaluated according to the *Sa* values, shows the worst surface roughness results. On the other hand, test 2.8, also performed under *cryogenic cooling* conditions, shows a significantly higher average value (3.85 μm) caused by the highest point value found in the tests, this value was taken at the exit of the titanium plate (15.45 μm).

Among the lines of work proposed to continue progressing in this research is the study of the influence of the sustainable cooling analysed on re-drilling burrs and on the tool degradation. In addition, the design of new specimens that allow the complete measurement of surface roughness to be carried out using a single measuring device and, in this way, further study the use of aerial-based response variables and their relationship with profile-based variables.

Funding

This work has been financed in part by the Spanish Ministry of Science. Innovation and Universities (Project RTI2018–102215-B-I00), by the Industrial Engineering School-UNED (REF2022-ICF04) and by the Master in Advanced Manufacturing Engineering.

Declaration of Competing Interest

The authors declare that they have no known competing financial interests or personal relationships that could have appeared to influence the work reported in this paper.

Data availability

No data was used for the research described in the article.

Acknowledgements

The authors thank the support given by the Industrial Production and Manufacturing Engineering (IPME) Research Group and by the Master of Manufacturing Advanced Engineering. The authors thank Grupo Antolín for providing part of the material with which the specimens were made.

References

[1] Intergovernmental Panel on Climate Change (IPCC): Summary for Policymakers n. d. https://www.ipcc.ch/site/assets/uploads/sites/2/2019/05/SR15_SPM_version_report_LR.pdf (accessed January 9, 2022).
[2] European Aviation Environmental Report 2019 n.d. https://ec.europa.eu/transport/siteshttps://www.easa.europa.eu/eaer/system/files/usr_uploaded/219473_EASA_EAER_2019_WEB_HI-RES_190311.pdf (accessed January 9, 2022).

[3] European Commission: Driving Clean Mobility n.d. https://ec.europa.eu/commission/presscorner/detail/en/MEMO_17_4243 (accessed October 26, 2020).
[4] ACARE n.d. https://www.acare4europe.org/sites/acare4europe.org/files/document/Flightpath2050_Final.pdf (accessed May 12, 2021).
[5] Reducing emissions from shipping sector n.d. https://ec.europa.eu/clima/policies/transport/shipping_en (accessed November 2, 2020).
[6] Boeing. Boeing Environment Report 2020 n.d. http://www.boeing.com/resources/boeingdotcom/principles/environment/pdf/er-companion-summary-092820.pdf (accessed March 19, 2021).
[7] Airbus Environment n.d. https://www.airbus.com/content/dam/corporate-topics/corporate-social-responsibility/environment/Environment-matters-for-the-future-of-aerospace.pdf (accessed March 19, 2021).
[8] 2020 Boeing Global Environment Report n.d. http://www.boeing.com/principles/environment/index.page (accessed July 3, 2022).
[9] Airbus Sustainability. Decarbonisation n.d. https://www.airbus.com/company/sustainability/environment/climate-change/decarbonisation.html (accessed July 3, 2022).
[10] Airbus, product responsability n.d. https://www.airbus.com/company/sustainability/environment/product-responsibility.html (accessed March 19, 2021).
[11] Li D, Chrysanthou A, Patel I, Williams G. Self-piercing riveting-a review. Int J Adv Manuf Technol 2017;92:1777–824. https://doi.org/10.1007/s00170-017-0156-x.
[12] Rubio EM, Blanco D, Marín MM, Carou D. Analysis of the latest trends in hybrid components of lightweight materials for structural uses. Procedia Manuf 2019;41:1047–54. https://doi.org/10.1016/j.promfg.2019.10.032.
[13] Gullino A, Matteis P, D'Aiuto F. Review of aluminum-to-steel welding technologies for car-body applications. Metals 2019:9. https://doi.org/10.3390/met9030315.
[14] Nassirnia M, Heidarpour A, Zhao XL, Minkkinen J. Innovative hollow columns comprising corrugated plates and ultra high-strength steel tubes. Thin-Walled Struct 2016;101:14–25. https://doi.org/10.1016/j.tws.2015.12.020.
[15] Mavhungu S.T., Akinlabi E.T., Onitiri M.A., Varachia F.M. Aluminum Matrix Composites for Industrial Use: Advances and Trends. Int Conf Sustain Mater Process Manuf (SMPM 2017), vol. 7, 2017, p. 178–82. https://doi.org/10.1016/j.promfg.2016.12.045.
[16] Talla G, Sahoo DK, Gangopadhyay S, Biswas CK. Modeling and multi-objective optimization of powder mixed electric discharge machining process of aluminum/alumina metal matrix composite. Eng Sci Technol Int J 2015;18:369–73. https://doi.org/10.1016/j.jestch.2015.01.007.
[17] Rubio EM, Villeta M, Valencia JL, Sáenz de Pipaon JM. Cutting parameter selection for efficient and sustainable repair of holes made in hybrid Mg-Ti-Mg component stacks by dry drilling operations. Materials 2018:11. https://doi.org/10.3390/ma11081369.
[18] Prime MB, Newborn MA, Balog JA. Quenching and cold-work residual stresses in aluminum hand forgings: contour method measurement and FEM prediction. Mater Sci Forum 2003;426–432:435–40. https://doi.org/10.4028/www.scientific.net/msf.426-432.435.
[19] Liu BY, Liu F, Yang N, Zhai XB, Zhang L, Yang Y, et al. Large plasticity in magnesium mediated by pyramidal dislocations. Science 2019;364:73–5. https://doi.org/10.1126/science.aaw2843.
[20] Xu J, Mkaddem A, El Mansori M. Recent advances in drilling hybrid FRP/Ti composite: a state-of-the-art review. Compos Struct 2016;135:316–38. https://doi.org/10.1016/j.compstruct.2015.09.028.
[21] Salama A, Li L, Mativenga P, Whitehead D. TEA CO_2 laser machining of CFRP composite. Appl Phys A-Mater Sci Process 2016:122. https://doi.org/10.1007/s00339-016-0025-8.
[22] Blanco D., Rubio E.M., Marín M.M., Camacho A.M. Sustainable and advanced manufacturing processes of light structural materials of the transport sector. In: Proceedings of the 9th Manufacturing Engineering Society International Conference (MESIC 2021) 23rd-25th June 2021, Gijón, Spain, vol. 1193, n.d., p. 1–9. https://doi.org/10.1088/1757–899X/1193/1/012126.
[23] Soo VK, Peeters J, Paraskevas D, Compston P, Doolan M, Duflou JR. Sustainable aluminium recycling of end-of-life products: a joining techniques perspective. J Clean Prod 2018;178:119–32. https://doi.org/10.1016/j.jclepro.2017.12.235.
[24] Lahdo R., Springer A., Pfeifer R., Kaierle S., Overmeyer L. High-power laser welding of thick steel-aluminum dissimilar joints. In: Proceedings of the 9th International Conference on Photonics, Optics and Laser Technology, vol. 83, 2016, p. 396–405. https://doi.org/10.1016/j.phpro.2016.08.041.
[25] Cirillo P, Marino A, Natale C, Di Marino E, Chiacchio P, De Maria G. A low-cost and flexible solution for one-shot cooperative robotic drilling of aeronautic stack materials. IFAC Pap 2017;50:4602–9. https://doi.org/10.1016/j.ifacol.2017.08.1013.
[26] Rubio EM, Villeta M, Valencia JL, Sáenz, de Pipaon JM. Experimental study for improving the repair of magnesium-aluminium hybrid parts by turning processes. Metals 2018:8. https://doi.org/10.3390/met8010059.
[27] Suhaimi MA, Yang G-D, Park K-H, Hisam MJ, Sharif S, Kim D-W. Effect of cryogenic machining for titanium alloy based on indirect, internal and external spray system. Procedia Manuf 2018;17:158–65. https://doi.org/10.1016/j.promfg.2018.10.031.
[28] García-Martínez E, Miguel V, Martínez-Martínez A, Manjabacas MC, Coello J. Sustainable lubrication methods for the machining of titanium alloys: an overview. Materials 2019;12:3852. https://doi.org/10.3390/ma12233852.
[29] Xu J, El Mansori M. Wear characteristics of polycrystalline diamond tools in orthogonal cutting of CFRP/Ti stacks. Wear 2017;376–377:91–106. https://doi.org/10.1016/j.wear.2016.11.038.
[30] Sun Y, Huang B, Puleo DA, Jawahir IS. Enhanced machinability of Ti-5553 alloy from cryogenic machining: comparison with MQL and flood-cooled machining and modeling. Procedia CIRP 2015;31:477–82. https://doi.org/10.1016/j.procir.2015.03.099.
[31] Kumar MS, Prabukarthi A, Krishnaraj V. Study on tool wear and chip formation during drilling carbon fiber reinforced polymer (CFRP)/titanium alloy (Ti6Al4V) stacks. Procedia Eng 2013. https://doi.org/10.1016/j.proeng.2013.09.133.
[32] Upadhyay N. Environmentally friendly machining: vegetable based cutting fluid. SAMRIDDHI: J Phys Sci Eng Technol 2015:7. https://doi.org/10.18090/samriddhi.v7i2.8630.
[33] Gómez-Parra A, Sanz A, Gamez AJ. Evaluation of the functional performance in turned workpieces: methodology and application to UNS A92024-T3. Materials 2018:11. https://doi.org/10.3390/ma11081264.
[34] Dimitrov D, Uheida E, Oosthuizen G, Blaine D, Laubscher R, Sterzing A, et al. Manufacturing of high added value titanium components. A South African perspective. IOP Conf Ser Mater Sci Eng 2018;430:012009. https://doi.org/10.1088/1757-899X/430/1/012009.
[35] Berzosa F, de Agustina B, Rubio EM. Tool selection in drilling of magnesium UNSM11917 pieces under dry and MQL conditions based on surface roughness. Procedia Eng 2017;184:117–27. https://doi.org/10.1016/j.proeng.2017.04.076.
[36] Zeng Z, Nie JF, Xu SW, Davies CHJ, Birbilis N. Super-formable pure magnesium at room temperature. Nat Commun 2017:8. https://doi.org/10.1038/s41467-017-01330-9.
[37] Muralidhar A, Narendranath S, Shivananda Nayaka H. Effect of equal channel angular pressing on AZ31 wrought magnesium alloys. J Magnes Alloy 2013. https://doi.org/10.1016/j.jma.2013.11.007.
[38] Barry N, Hainsworth SV, Fitzpatrick ME. Effect of shot peening on the fatigue behaviour of cast magnesium A8. Mater Sci Eng A 2009;507:50–7. https://doi.org/10.1016/j.msea.2008.11.044.
[39] International Magnesium Association. Recycling Magnesium. n.d. https://www.intlmag.org/page/sustain_recycle_ima (accessed November 8, 2021).
[40] The Aluminum Association. Recycling. n.d. https://www.aluminum.org/industries/production/recycling (accessed November 5, 2020).
[41] Baldan A. Adhesion phenomena in bonded joints. Int J Adhes Adhes 2012;38:95–116. https://doi.org/10.1016/j.ijadhadh.2012.04.007.
[42] Caminero MA, Pavlopoulou S, Lopez-Pedrosa M, Nicolaisson BG, Pinna C, Soutis C. Analysis of adhesively bonded repairs in composites: damage detection and prognosis. Compos Struct 2013;95:500–17. https://doi.org/10.1016/j.compstruct.2012.07.028.
[43] Haghshenas M, Gerlich AP. Joining of automotive sheet materials by friction-based welding methods: a review. Eng Sci Technol Int J 2018;21:130–48. https://doi.org/10.1016/j.jestch.2018.02.008.
[44] Ojo SO, Ismail SO, Paggi M, Dhakal HN. A new analytical critical thrust force model for delamination analysis of laminated composites during drilling operation. Compos Part B-Eng 2017;124:207–17. https://doi.org/10.1016/j.compositesb.2017.05.039.
[45] Karpat Y, Deger B, Bahtiyar O. Drilling thick fabric woven CFRP laminates with double point angle drills. J Mater Process Technol 2012;212:2117–27. https://doi.org/10.1016/j.jmatprotec.2012.05.017.
[46] Kyratsis P., Garcia-Hernandez C., Vakondios D., Antoniadis A. Thrust force and torque mathematical models in drilling of Al7075 using the response surface methodology, 2016. https://doi.org/10.1007/978–3-319–23838-8_6.
[47] Zhang J, Pei ZJ. Characterization methods for surface integrity. Surf Integr Mach 2010. https://doi.org/10.1007/978-1-84882-874-2_4.
[48] Astakhov VP. Ecological machining: near-dry machining. Mach Fundam Recent Adv 2008. https://doi.org/10.1007/978-1-84800-213-5_7.
[49] Dixit US, Sarma DK, Davim JP. Green manufacturing. SpringerBriefs Appl Sci Technol 2012. https://doi.org/10.1007/978-1-4614-2308-9_1.
[50] Astakhov VP. Cutting tool sustainability. Sustain Manuf 2013. https://doi.org/10.1002/9781118621653.ch2.
[51] Sáenz de Pipaón JM. Diseño y fabricación de probetas de componentes híbridos con aleaciones de magnesio para ensayos de mecanizado. (Ph.D. thesis). UNED; 2013.
[52] Shokrani A, Dhokia V, Newman ST. Investigation of the effects of cryogenic machining on surface integrity in CNC end milling of Ti-6Al-4V titanium alloy. J Manuf Process 2016;21. https://doi.org/10.1016/j.jmapro.2015.12.002.
[53] Dixit US, Sarma DK, Davim JP. Machining with minimal cutting fluid. SpringerBriefs Appl Sci Technol 2012. https://doi.org/10.1007/978-1-4614-2308-9_2.
[54] Gupta MK, Song Q, Liu Z, Sarikaya M, Jamil M, Mia M, et al. Ecological, economical and technological perspectives based sustainability assessment in hybrid-cooling assisted machining of Ti-6Al-4 V alloy. Sustain Mater Technol 2020:26. https://doi.org/10.1016/j.susmat.2020.e00218.
[55] Dixit US, Sarma DK, Davim JP. Economics of environmentally friendly machining. SpringerBriefs Appl Sci Technol. Springer Verlag,; 2012. p. 77–80. https://doi.org/10.1007/978-1-4614-2308-9_7.
[56] Fratila D. Sustainable manufacturing through environmentally-friendly machining, 2013. https://doi.org/10.1007/978–3-642–33792-5_1.
[57] Carou D, Rubio EM, Davim JP. A note on the use of the minimum quantity lubrication (MQL) system in turning. Ind Lubr Tribol 2015;67:256–61. https://doi.org/10.1108/ILT-07-2014-0070.
[58] Carou D, Rubio EM, Lauro CH, Davim JP. The effect of minimum quantity lubrication in the intermittent turning of magnesium based on vibration signals. Meas J Int Meas Confed 2016;94:338–43. https://doi.org/10.1016/j.measurement.2016.08.016.
[59] Gaitonde VN, Karnik SR, Davim JP. Optimal mql and cutting conditions determination for desired surface roughness in turning of brass using genetic

algorithms. Mach Sci Technol 2012;16. https://doi.org/10.1080/10910344.2012.673976.
[60] Dixit US, Sarma DK, Davim JP. Gas-cooled machining. SpringerBriefs Appl Sci Technol 2012. https://doi.org/10.1007/978-1-4614-2308-9_4.
[61] Dixit US, Sarma DK, Davim JP. A detailed comparison of dry and air-cooled turning. SpringerBriefs Appl Sci Technol 2012. https://doi.org/10.1007/978-1-4614-2308-9_5.
[62] Sarma DK, Dixit US. A comparison of dry and air-cooled turning of grey cast iron with mixed oxide ceramic tool. J Mater Process Technol 2007;190. https://doi.org/10.1016/j.jmatprotec.2007.02.049.
[63] Singaravel B, Shekar KC, Reddy GG, Prasad SD. Experimental investigation of vegetable oil as dielectric fluid in Electric discharge machining of Ti-6Al-4V. Ain Shams Eng J 2020;11:143–7. https://doi.org/10.1016/j.asej.2019.07.010.
[64] Krolczyk GM, Maruda RW, Krolczyk JB, Wojciechowski S, Mia M, Nieslony P, et al. Ecological trends in machining as a key factor in sustainable production – a review. J Clean Prod 2019;218:601–15. https://doi.org/10.1016/j.jclepro.2019.02.017.
[65] Rezende BA, Silveira ML, Vieira LMG, Abrao AM, de Faria PE, Campos Rubio JC. Investigation on the effect of drill geometry and pilot holes on thrust force and burr height when drilling an aluminium/PE sandwich material. Materials 2016:9. https://doi.org/10.3390/ma9090774.
[66] Struzikiewicz G, Sioma A. Evaluation of surface roughness and defect formation after the machining of sintered aluminum alloy AlSi10Mg. Materials 2020:13. https://doi.org/10.3390/ma13071662.
[67] Blanco D., Rubio E.M., Marín M.M., Davim J.P. Advanced materials and multi-materials applied in aeronautical and automotive fields: a systematic review approach. In: Proceedings of the 14th CIRP Conference on Intelligent Computation in Manufacturing Engineering Gulf Naples, Italy 2020;99:196–201. https://doi.org/10.1016/J.PROCIR.2021.03.027.
[68] Petropoulos GP, Pandazaras CN, Davim JP. Surface texture characterization and evaluation related to machining. Surf Integr Mach 2010. https://doi.org/10.1007/978-1-84882-874-2_2.
[69] The American Society of Mechanical Engineers. Surface Texture: Surface Roughness, Waviness and Lay; ANSI/ASME B461–2009; ASME 2010.
[70] Gao H, Ma B, Singh RP, Yang H. Areal surface roughness of AZ31B magnesium alloy processed by dry face turning: An experimental framework combined with regression analysis. Materials 2020:13. https://doi.org/10.3390/ma13102303.
[71] Harcarik M, Jankovych R. Relationship between values of profile and areal surface texture parameters. MM Sci J 2016;2016. https://doi.org/10.17973/MMSJ.2016_12_2016206 (1659–62).
[72] Blanco D, Rubio EM, Lorente-Pedreille RM, Saénz-Nuño MA. Lightweight structural materials in open access: latest trends. Materials 2021;14:6577. https://doi.org/10.3390/ma14216577.
[73] Blanco D, Rubio EM, Marín MM, Davim JP. Repairing hybrid Mg-Al-Mg components using sustainable cooling systems. Materials 2020:13. https://doi.org/10.3390/ma13020393.
[74] Blanco D, Rubio EM, Sáenz de Pipaón JM, Marín MM. Thicknesses/roughness relationship in mg-al-mg and mg-ti-mg hybrid component plates for drilled aeronautical lightweight parts. Appl Sci 2020;10:1–20. https://doi.org/10.3390/app10228208.
[75] López De Lacalle LN, Angulo C, Lamikiz A, Sánchez JA. Experimental and numerical investigation of the effect of spray cutting fluids in high speed milling. J Mater Process Technol 2006:172. https://doi.org/10.1016/j.jmatprotec.2005.08.014.
[76] Astakhov VP, Davim JP. Tools (geometry and material) and tool wear. Mach Fundam Recent Adv 2008. https://doi.org/10.1007/978-1-84800-213-5_2.
[77] Rubio EM, Valencia JL, De Agustina B, Saá AJ. Tool selection based on surface roughness in dry facing repair operations of magnesium pieces. Int J Mater Prod Technol 2014;48:116–34. https://doi.org/10.1504/IJMPT.2014.059021.